



Contents lists available at ScienceDirect

# Journal of Sound and Vibration

journal homepage: [www.elsevier.com/locate/jsvi](http://www.elsevier.com/locate/jsvi)

## Optimal designs for non-uniform tuned liquid column dampers in horizontal motion

Jong-Cheng Wu<sup>\*</sup>, Cheng-Hsing Chang, Yuh-Yi Lin

Department of Civil Engineering, Tamkang University, Taipei, Taiwan

### ARTICLE INFO

#### Article history:

Received 13 November 2008

Received in revised form

14 April 2009

Accepted 18 April 2009

Handling Editor: L.G. Tham

Available online 21 May 2009

### ABSTRACT

In this paper, the optimal design parameters of tuned liquid column dampers (TLCD) with non-uniform cross-sections for application to a SDOF structure in horizontal motion are summarized. In the first part, optimization for the interacted structure subjected to harmonic loading is revisited and the computation is facilitated by a non-iterative analytical response solution (closed-form solution) proposed for expediting the process. From both analytical and numerical inspections, some new findings were clearly observed, including (i) the optimal head loss is inversely proportional to excitation amplitude; while the optimal frequency tuning ratio is independent of the excitation level; (ii) the minimal peak amplitude of the structure over all possible frequencies occurs when the two resonant peaks in the structural response are equal, and this applies to both damped and undamped structures; (iii) a uniform TLCD is always the best choice under the same condition of structural damping, mass ratio and horizontal length ratio of the TLCD; and (iv) the optimal performance is the same for the cases with reciprocal cross-section ratios. Based on the conclusion in the first part, the second part presents design tables containing lists of optimal parameters for non-uniform (cross-section ratios 2 and  $\frac{1}{2}$ ) and uniform TLCDs as quick guidelines for practical use. For completeness, these tables were also incorporated with the optimal parameters for TLCDs under a white-noise type of loading, which are excerpted from a previously published research. Some results of parametric studies observed from the design tables were also addressed. Finally, a design example is used to demonstrate the use of these design tables.

© 2009 Elsevier Ltd. All rights reserved.

### 1. Introduction

In recent years, the newly developed construction technologies toward lighter and stronger materials have facilitated the realization of more and more high-rise buildings in many urban areas where space usage is demanding. The typical examples are the Petronas Twin Tower (452 m) in Kuala Lumpur, Malaysia, and Taipei 101 Building (508 m) in Taipei, Taiwan and the under-construction super-high building—Burj Dubai (807.7 m) in Dubai. However, the down side with it is the high susceptibility of their responses to wind loading, especially the induced acceleration magnification frequently causes occupants' discomfort. Thus, for structures such as these, it is very desirable to use control devices for the sake of vibration suppression. Among many varieties of control devices, the tuned liquid column damper (termed as TLCD) that is composed of fluid in a U-shape of liquid column container is a good candidate. During a motion, this device can dissipate

<sup>\*</sup> Corresponding author. Tel.: +886 2 26215656x2758; fax: +886 2 26209747.

E-mail address: [joncheng@mail.tku.edu.tw](mailto:joncheng@mail.tku.edu.tw) (J.-C. Wu).

Nomenclature			
$A_h$	cross-sectional area in the horizontal column of a TLCD	$\hat{x} = x/L_h$	non-dimensional $x$
$A_v$	cross-sectional area in the vertical column of a TLCD	$\hat{x}_0$	amplitude of a harmonic $\hat{x}$
$C_0, C_2, C_3, C_4$	coefficients defined in Eq. (17)	$\hat{x}_{p(\text{original})}$	original structural peak amplitude over all possible frequencies
$F$	wind load on the structure	$[\hat{x}_0]_{\text{norm}}$	normalized $\hat{x}_0$
$\hat{F} = FT_d^2/ML_h$	non-dimensional $F$	$[\hat{x}_p]_{\text{norm}}$	peak amplitude of $[\hat{x}_0]_{\text{norm}}$ over all possible frequencies
$g$	acceleration due to gravity	$y$	displacement of the liquid surface
$G$	coefficient defined in Eq. (11)	$\hat{y} = y/L_h$	non-dimensional $y$
$k = \omega/\omega_d$	non-dimensional excitation frequency	$\hat{y}_0$	amplitude of a harmonic $\hat{y}$
$k_1, k_2, k_3$	three frequencies as defined in Fig. 5	$[\hat{y}_0]_{\text{norm}}$	normalized $\hat{y}_0$
$L = 2L_v + L_h$	total length of the liquid column of a TLCD	$[\hat{y}_p]_{\text{norm}}$	peak amplitude of $[\hat{y}_0]_{\text{norm}}$ over all possible frequencies
$L_e = 2L_v + vL_h$	effective length of the liquid column of a TLCD	$\beta_1 = \omega_s/\omega_d$	frequency tuning ratio of the structure versus TLCD
$L_h$	horizontal column length of a TLCD	$\beta_{1\text{opt}}$	optimal frequency tuning ratio
$L_v$	vertical column length of a TLCD	$\eta$	head loss coefficient
$m = vp/(v+p(1-v))$	parameter related to $v$ and $p$	$\eta_{\text{opt}}$	optimal head loss coefficient
$M, C, K$	structural mass, damping and stiffness constants	$\mu = \rho A_h(L_h + 2vL_v)/M$	mass ratio of the liquid versus structure
$n = p/(1-p(1-v))$	parameter related to $v$ and $p$	$v = A_v/A_h$	cross-sectional ratio of the vertical column versus horizontal column
$p = L_h/L$	ratio of the horizontal length to total length of the liquid column	$\xi = C/2M\omega_s$	damping ratio of the structure
$t$	time	$\xi_e$	effective damping ratio of the structure equipped with a TLCD
$\hat{t} = t/T_d$	non-dimensional $t$	$\rho$	fluid density
$T_A, T_B, T_C, T_D, T_E, T_F$	coefficients defined in Eqs. (12) and (15)	$\varphi_y$	amplitude of a harmonic $y$
$T_{\hat{x}\hat{F}}$	frequency response function of $\hat{x}$ induced by $\hat{F}$	$\varphi_{\hat{y}} = \varphi_y/L_h$	non-dimensional $\varphi_y$
$T_{\hat{y}\hat{F}}$	frequency response function of $\hat{y}$ induced by $\hat{F}$	$\omega$	excitation frequency
$T_d = 2\pi\sqrt{L_e/2g}$	natural period of a TLCD	$\omega_d = \sqrt{2g/L_e}$	natural frequency of a TLCD
$x$	displacement of the structure equipped with a TLCD	$\omega_s = \sqrt{K/M}$	natural frequency of the structure

energy by the relative movement of the fluid passing through an orifice located in the liquid column. In terms of advantages over other types of energy-dissipating dampers, the properties of TLCD (such as the natural frequency and damping) can be reliably and precisely determined from the length of the liquid column and the orifice size.

The original idea of TLCD was developed by Sakai et al. [1] for suppression of horizontal motion of structures. After that, quite a few research papers, namely Xu et al. [2], Hitchcock et al. [3], Balendra et al. [4], Min et al. [5] and Felix et al. [6], have verified its effectiveness for suppressing wind-induced horizontal responses, among whom Hitchcock et al. [3] even investigated a general type of TLCDs that have non-uniform cross-sections in the horizontal and vertical columns, termed as liquid column vibration absorber (LCVA). Recently, the application of TLCDs was further extended to the suppression of pitching motion for bridge decks (e.g., Xue et al. [7] and Wu et al. [8]). For the application to the control of horizontal motion toward implementation, some researchers have spent efforts on determining optimal TLCD designs, such as Chang et al. [9] and Chang [10] on undamped structures, Wu et al. [11] on damped structures, and Yalla et al. [12] on both damped and undamped structures. Their results of optimal parameters were provided for the situation when the loading on buildings is of a white-noise type, such as wide-banded along-wind loads. As for the across-wind loading which is more likely to be of a harmonic type due to the vortex shedding effect (see Simiu and Scanlan [13]), the investigation of optimal parameters can only be found in Gao et al. [14] to date. However, it contains quite limited results because of the cumbersome computation performed by using direct simulation in the time domain. Performing such computation in the optimization process is not practically feasible.

To gain more understanding on the optimal TLCD design, the first part of this paper revisits the optimal parametric investigation for TLCDs under a harmonic type of wind loading. From literature review, the conventional approach for obtaining the optimal parameters of an undamped structure equipped with a tuned mass damper (TMD) is to use the idea of invariant points of the structural amplitude in the frequency domain [15]. The optimal frequency tuning ratio can be determined by equating the amplitudes at the two invariant points, and the optimal damping ratio of the damper can be obtained by averaging the two damping ratios that make the amplitude at the individual invariant point as flat as possible (i.e., a local maximum occurs at the invariant point). For a damped structure, the above approach is no longer applicable

because of inexistence of invariant points. In such a case, the optimal parameters can be determined by the numerical optimization that directly minimizes the structural amplitude over all possible frequencies. In the TLCD application, due to the fact that the TLCD damping is response-dependent (dependent on the liquid amplitude even if the damping term is linearized), it is more straightforward to use direct optimization even though there still exist invariant points (see Section 4.2) in this approach for undamped structures.

Therefore, in this paper, the optimization is performed by directly minimizing the peak structural amplitude over all possible frequencies using a non-iterative analytical response solution (closed-form solution) that was specifically derived for harmonic loading to facilitate computation. In this way, the optimal parameters, such as the optimal tuning ratio and head loss coefficient, and some other practically related information for design can be subsequently determined.

Based on the conclusion in the first part, the second part presents the design tables containing the complete lists of the optimal parameters for both uniform ( $\nu = 1$ ) and non-uniform ( $\nu = 2$  and  $\frac{1}{2}$ ) TLCDs as quick guidelines for practical use. These tables were also incorporated with the optimal parameters for TLCDs under a white-noise type of loading, which were excerpted from a previous research by the authors [11]. Finally, a design example will be used to demonstrate the use of these design tables.

**2. Interaction equations in horizontal motion**

The schematic diagram of a single-degree-of-freedom structure equipped with a TLCD in horizontal motion is shown in Fig. 1. For generality, the cross-sections in horizontal and vertical columns of a TLCD can be non-uniform, depending on the choice of the designer. Some presumptions for TLCDs in deriving the equations of motion include: (i) the fluid is incompressible (i.e., the flow rate is constant), depicting that water is a good choice; (ii) the sloshing behavior on the liquid surface is negligible (this is considerably satisfied when the structural frequency is as low as 0.5 Hz or even lower, which is quite common for high-rise buildings); (iii) the in-plane width of the TLCD vertical column cross-section should be much smaller than its horizontal length.

By using Lagrange’s equations and energy principles, the interaction equations of motion for the structure and liquid surface motion in a TLCD can be expressed as (e.g., Chang et al. [9], Gao et al. [14])

$$M\ddot{x} + \rho A_h(2\nu L_v + L_h)\dot{\ddot{x}} + \rho A_h \nu L_h \dot{y} + C\dot{x} + Kx = F(t) \tag{1}$$

and

$$\rho A_h \nu L_e \dot{y} + \rho A_h \nu L_h \ddot{x} + (1/2)\rho A_h \nu^2 \eta |\dot{y}| \dot{y} + 2\rho A_h g \nu y = 0, \tag{2}$$

respectively. A brief derivation can be referred to Appendix A for readers’ interest. In Eqs. (1) and (2),  $x$  and  $y$  denote displacements of the structure and liquid surface, respectively;  $M$ ,  $C$ ,  $K$  are structural mass, damping and stiffness constants;  $F(t)$  is external loading;  $L_h$  and  $L_v$  are horizontal and vertical column lengths;  $A_h$  and  $A_v$  are cross-sectional areas in horizontal and vertical columns, respectively;  $\rho$  is fluid density;  $g$  is acceleration due to gravity;  $\nu = A_v/A_h$  is cross-sectional ratio of the vertical column versus horizontal column;  $L_e = 2L_v + \nu L_h$  is defined as the effective length; and  $\eta$  is head loss coefficient. The head loss can be considered as the overall head loss induced by flow motion in the liquid column, although it is mainly induced by the flow passing through the orifice. The effective length  $L_e$  will be the total length  $L = 2L_v + L_h$  of the liquid column at  $\nu = 1$ . From Eq. (2), it is easily observed that the natural frequency of a TLCD is  $\omega_d = \sqrt{2g/L_e}$  rad/s, and the natural period is  $T_d = 2\pi\sqrt{L_e/2g}$  seconds accordingly.

For a multiple-degree-of-freedom system with a specified mode to be controlled, the modal equation should be obtained by performing modal decomposition with the mode shape component at the location where the TLCD is installed set to one. Then the corresponding modal mass, damping and stiffness will be used as the structural properties  $M$ ,  $C$ ,  $K$  in the formula described above.

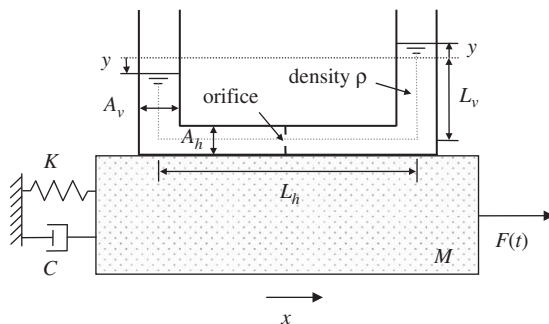


Fig. 1. SDOF damped structure equipped with TLCD under external load.

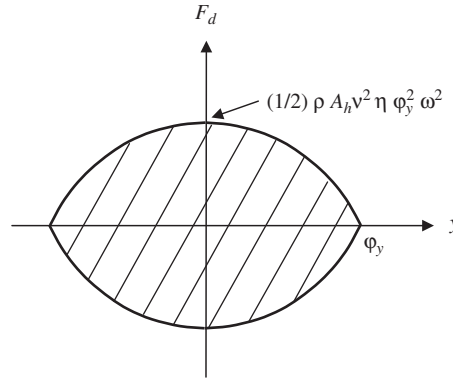


Fig. 2. Hysteretic loop of the damping force in a TLCD.

### 2.1. Non-dimensionalization

For conciseness of analysis and a better presentation, the equations of motion in Eqs. (1) and (2) were non-dimensionalized before further derivation. Thus, the resultant forms of the non-dimensionalized equations (1) and (2) can be expressed as

$$(1 + \mu)\hat{x}'' + \mu m \hat{y}'' + 4\pi \zeta \beta_1 \hat{x}' + 4\pi^2 \beta_1^2 \hat{x} = \hat{F}(\hat{t}) \tag{3}$$

$$\hat{y}'' + n \hat{x}'' + \frac{1}{2} v n \eta \hat{y}' |\hat{y}'| + 4\pi^2 \hat{y} = 0 \tag{4}$$

in which the dimensionless variables are defined as  $\hat{x} = x/L_h$ ;  $\hat{y} = y/L_h$ ;  $\hat{t} = t/T_d$ ;  $\hat{F} = FT_d^2/ML_h$ ;  $\zeta = C/2M\omega_s$  is damping ratio of the structure with  $\omega_s = \sqrt{K/M}$  being the natural frequency of the structure;  $\beta_1 = \omega_s/\omega_d$  is frequency tuning ratio of the structure versus TLCD;  $p = L_h/L$  is ratio of the horizontal length to total length of the liquid column;  $\mu = \rho A_h(L_h + 2vL_v)/M$  is mass ratio of the liquid versus structure;  $m$  and  $n$  are two parameters related to  $p$  and  $v$ , defined as  $n = p/(1-p(1-v))$  and  $m = vp/(v+p(1-v))$ . In fact, the value of  $n$  is the ratio of  $L_h$  versus  $L_e$ , while  $m$  is the ratio of  $vL_h$  versus  $(L_h+2vL_v)$ . Accordingly, the total length  $L$  can be expressed as  $L = nL_e/p = L_e/(1-p(1-v))$ . Note that in Eqs. (3) and (4), the notation prime (') represents the differentiation with respect to the dimensionless time  $\hat{t}$ .

### 2.2. Equivalent damping for a harmonic type of loading

Under a harmonic type of loading with a frequency  $\omega$ , an equivalent viscous damping in the form of  $(4/3\pi)\rho A_h v^2 \eta \varphi_y \omega \dot{y}$  ( $\varphi_y$  is the amplitude of  $y$ ) can be used to replace the damping term  $(\frac{1}{2})\rho A_h v^2 \eta |\dot{y}| \dot{y}$  in Eq. (2) by a stochastic approach [14]. Alternatively it can be obtained by equating the dissipated energy from both damping expressions within a cycle as follows. Let the harmonic response  $y$  be expressed by  $y = \varphi_y \sin \omega t$  in which  $\varphi_y$  is the amplitude of  $y$ , then the damping force can be written as  $F_d = (\frac{1}{2})\rho A_h v^2 \eta |\dot{y}| \dot{y} = (\frac{1}{2})\rho A_h v^2 \eta \varphi_y^2 \omega^2 \cos \omega t \cdot |\cos \omega t|$ . The hysteretic loop of such a damping force in a full cycle was plotted in Fig. 2 for illustration. In the first quarter cycle, the relation between  $y$  and  $F_d$  is obtained as

$$\frac{F_d}{(1/2)\rho A_h v^2 \eta \varphi_y^2 \omega^2} = 1 - \left(\frac{y}{\varphi_y}\right)^2 \tag{5}$$

Hence, the dissipated energy by the damping force in the quarter cycle is the area from 0 to  $\varphi_y$  under the  $F_d$  curve. The resulting dissipated energy in a full cycle is integrated to be  $(\frac{4}{3})\rho A_h v^2 \eta \omega^2 \varphi_y^3$ . Equating this to the dissipated energy  $\pi C_{eq} \omega \varphi_y^2$  caused by the equivalent viscous damping force  $C_{eq} \dot{y}$  leads to

$$C_{eq} = (4/3\pi)\rho A_h v^2 \eta \omega \varphi_y \tag{6}$$

With the damping term in Eq. (4) replaced by  $C_{eq} \dot{y}$ , the non-dimensionalized equation can be expressed as

$$\hat{y}'' + n \hat{x}'' + (8/3)v n \eta \varphi_{\hat{y}} k \hat{y}' + 4\pi^2 \hat{y} = 0 \tag{7}$$

in which  $k = \omega/\omega_d$  is dimensionless excitation frequency; and  $\varphi_{\hat{y}} = \varphi_y/L_h$  is the dimensionless amplitude of  $y$ . The accuracy of such an approximation will be verified in the numerical simulation presented in Section 3.

### 3. Analytical solution to harmonic loading

This section gives the derivation of the analytical solution of the interaction equations (3) and (7). By replacing  $\hat{x}$ ,  $\hat{y}$  and  $\hat{F}(\hat{t})$  in Eqs. (3) and (7) by the complex harmonic functions  $\hat{x}_0 e^{i2\pi k \hat{t}}$ ,  $\hat{y}_0 e^{i2\pi k \hat{t}}$  and  $\hat{F}_0 e^{i2\pi k \hat{t}}$  ( $i = \sqrt{-1}$ ), respectively, the

complex amplitude  $\hat{x}_0$  and  $\hat{y}_0$  can be obtained as functions of the force amplitude  $\hat{F}_0$ , i.e.,

$$\hat{x}_0 = T_{\hat{x}\hat{F}} \hat{F}_0 \quad (8)$$

$$\hat{y}_0 = T_{\hat{y}\hat{F}} \hat{F}_0 \quad (9)$$

in which  $T_{\hat{x}\hat{F}}$  and  $T_{\hat{y}\hat{F}}$  represent the frequency response functions of  $\hat{x}$  and  $\hat{y}$  induced by  $\hat{F}$ , i.e.,

$$T_{\hat{x}\hat{F}} = \frac{(1 - k^2) + i \left( \frac{4}{3\pi} k^2 v n \eta \varphi_{\hat{y}} \right)}{G}; \quad T_{\hat{y}\hat{F}} = \frac{n k^2}{G} \quad (10)$$

with

$$G = (T_B + T_C \cdot \varphi_{\hat{y}}) + i(T_D + T_E \cdot \varphi_{\hat{y}}) \quad (11)$$

$$T_B = 4\pi^2(1 - k^2)[\beta_1^2 - k^2(1 + \mu)] - 4\pi^2 k^4 \mu m n; \quad T_C = -\frac{32}{3}\pi k^3 v n \eta \xi \beta_1;$$

$$T_D = 8\pi^2 k \xi \beta_1 (1 - k^2); \quad T_E = \frac{16}{3}\pi k^2 v n \eta [\beta_1^2 - k^2(1 + \mu)] \quad (12)$$

By using the relation  $\varphi_{\hat{y}} = |\hat{y}_0|$ , the substitution of Eqs. (10)–(12) into square of the absolute value on both sides of Eqs. (8) and (9) leads to

$$|\hat{x}_0|^2 = \frac{T_F \cdot \hat{F}_0^2}{(T_B + T_C \cdot |\hat{y}_0|)^2 + (T_D + T_E \cdot |\hat{y}_0|)^2} \quad (13)$$

$$|\hat{y}_0|^2 = \frac{T_A \cdot \hat{F}_0^2}{(T_B + T_C \cdot |\hat{y}_0|)^2 + (T_D + T_E \cdot |\hat{y}_0|)^2} \quad (14)$$

in which

$$T_F = (1 - k^2)^2 + \left( \frac{4}{3\pi} k^2 v n \eta |\hat{y}_0| \right)^2; \quad T_A = n^2 k^4 \quad (15)$$

By further rearranging Eq. (14) into a polynomial equation in  $|\hat{y}_0|$  as

$$C_4 |\hat{y}_0|^4 + C_3 |\hat{y}_0|^3 + C_2 |\hat{y}_0|^2 + C_0 = 0 \quad (16)$$

in which

$$C_4 = T_C^2 + T_E^2; \quad C_3 = 2(T_B \cdot T_C + T_D \cdot T_E); \quad C_2 = T_B^2 + T_D^2; \quad C_0 = -T_A \cdot \hat{F}_0^2, \quad (17)$$

the value of  $|\hat{y}_0|$  can be solved analytically. Based on the extensive simulation from Eq. (17), it can be shown that  $|\hat{y}_0|$  has a unique positive or zero solution. Consequently, the frequency response functions  $T_{\hat{x}\hat{F}}$ ,  $T_{\hat{y}\hat{F}}$  and the amplitude  $|\hat{x}_0|$  can be obtained by substituting the solution of  $|\hat{y}_0|$  back into Eqs. (10) and (13), respectively. It should be noticed that the system is in fact not linear because both of the frequency response functions  $T_{\hat{x}\hat{F}}$  and  $T_{\hat{y}\hat{F}}$  are functions of  $\hat{F}_0$ .

To verify the accuracy of the approximation of damping term adopted in Eq. (7), extensive comparisons were made between the analytical solutions and those from direct simulation of the original form (Eqs. (3) and (4)) in time domain. Three cases out of many were demonstrated in Fig. 3, each case uses the cross-sectional ratio  $\nu$  equal to 1, 2 and  $\frac{1}{2}$ , respectively. As shown in Fig. 3, the comparisons were very satisfactory. However, the computation effort involved in the direct simulation of the original equations was way far cumbersome.

#### 4. Optimization and results

In this section, the optimization problem for a structure equipped with a TLCD under a harmonic load is first defined, and optimization is performed numerically to determine the optimal parameters.

##### 4.1. Performance index

In most civil engineering applications, the excitation frequency from harmonic disturbance (such as vortex shedding in the across-wind direction) usually varies and is not certain. Hence it is more reasonable to consider the worst case of structural response in all possible frequencies while response is minimized. Let the normalized structural and liquid responses be defined as

$$[\hat{x}_0]_{\text{norm}} = |\hat{x}_0| / \hat{x}_{p(\text{original})} \quad (18)$$

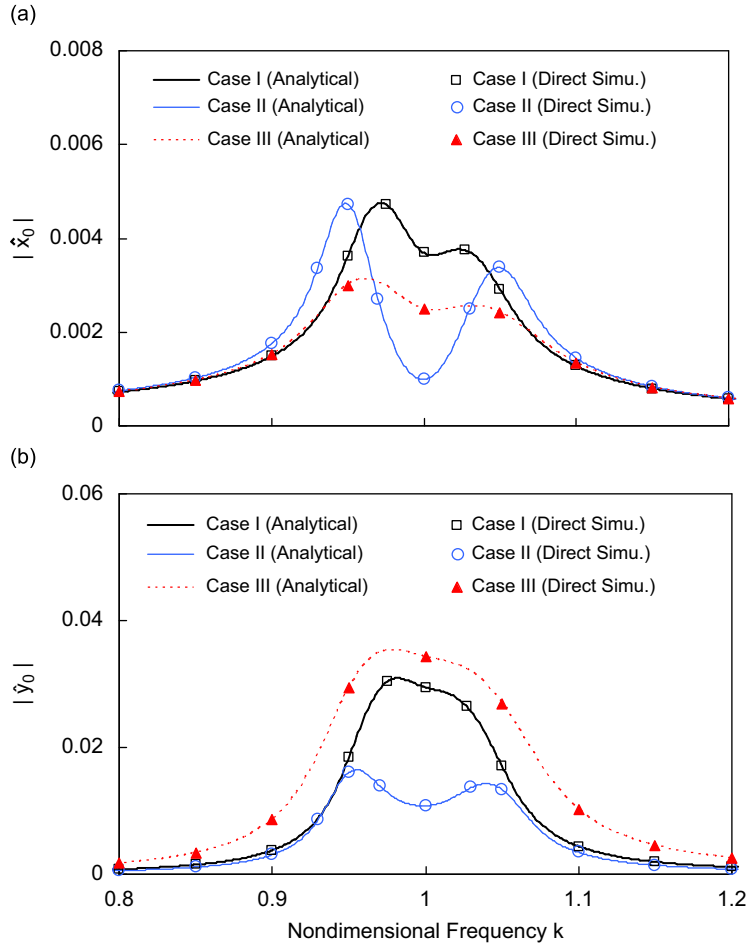


**Fig. 3.** Comparisons of the analytical solution and direct simulation in three cases (Case I:  $\nu = 1, \zeta = 1\%, \mu = 1\%, p = 0.6, \hat{F}_0 = 0.01, \eta = 10, \beta_1 = 1$ , Case II:  $\nu = 2, \zeta = 1\%, \mu = 2\%, p = 0.7, \hat{F}_0 = 0.01, \eta = 10, \beta_1 = 1$  and Case III:  $\nu = 0.5, \zeta = 2\%, \mu = 1\%, p = 0.8, \hat{F}_0 = 0.01, \eta = 10, \beta_1 = 1$ ): (a)  $\hat{x}_0$  versus  $k$  and (b)  $\hat{y}_0$  versus  $k$ .

and

$$[\hat{y}_0]_{\text{norm}} = |\hat{y}_0| / \hat{x}_{p(\text{original})} \tag{19}$$

in which  $\hat{x}_{p(\text{original})}$  is the original structural peak amplitude (worst case) over all possible frequencies. The value of  $\hat{x}_{p(\text{original})}$  can be derived from the equation of motion of the original structure, i.e., Eq. (3) with  $\mu$  set to zero, i.e.,

$$\hat{x}_{p(\text{original})} = \frac{\hat{F}_0}{4\pi^2\beta_1^2} \cdot \frac{1}{2\zeta\sqrt{1-\zeta^2}} \tag{20}$$

With this, the performance index (P.I.) is defined as the peak amplitude (worst case) of  $[\hat{x}_0]_{\text{norm}}$  over all possible frequencies, i.e.,

$$\text{P.I.} = [\hat{x}_p]_{\text{norm}} = \text{Max}_{k \in \mathbb{R}} [\hat{x}_0]_{\text{norm}} \tag{21}$$

According to this definition, the optimization (minimization) on the performance index can be categorized as a kind of the so-called Min–Max problem in which  $[\hat{x}_p]_{\text{norm}}$  is actually the  $H_\infty$  norm of  $[\hat{x}_0]_{\text{norm}}$  in Eq. (18) [16]. A smaller  $[\hat{x}_p]_{\text{norm}}$  represents a better performance.

In addition, the overall effective damping ratio  $\zeta_e$  for the structure can be calculated by equating  $[\hat{x}_p]_{\text{norm}} \cdot \hat{x}_{p(\text{original})}$  to  $(\hat{F}_0 / 4\pi^2\beta_1^2 \cdot 1 / 2\zeta_e \sqrt{1-\zeta_e^2})$ . The substitution of Eq. (20) leads to

$$\zeta_e^4 - \zeta_e^2 + \zeta^2(1-\zeta^2) / [\hat{x}_p]_{\text{norm}}^2 = 0 \tag{22}$$

Hence, the equivalent damping ratio  $\zeta_e$  can be obtained by

$$\zeta_e = \left( \frac{1 - \sqrt{1 - 4\zeta^2(1 - \zeta^2)/[\hat{x}_p]_{\text{norm}}^2}}{2} \right)^{1/2} \approx \frac{\zeta}{[\hat{x}_p]_{\text{norm}}} \tag{23}$$

A larger  $\zeta_e$  represents better performance.

Similarly, the normalized peak amplitude (worst case) of  $[\hat{y}_0]_{\text{norm}}$  over all possible frequencies can be also defined as

$$[\hat{y}_p]_{\text{norm}} = \text{Max}_{k \in R} [\hat{y}_0]_{\text{norm}} \tag{24}$$

The value of  $[\hat{y}_p]_{\text{norm}}$  is to be used for checking if the liquid surface displacement exceeds the length of the vertical liquid column.

4.2. Determination of optimal parameters  $\nu$ ,  $\eta$  and  $\beta_1$

As shown in Eqs. (13) and (18), the independent parameters for determining  $[\hat{x}_p]_{\text{norm}}$  include the structural damping ratio  $\zeta$ , mass ratio  $\mu$ , cross-sectional ratio  $\nu$ , horizontal length ratio  $p$ , non-dimensional force amplitude  $\hat{F}_0$ , head loss coefficient  $\eta$  and frequency tuning ratio  $\beta_1$ . Since the structural damping ratio  $\zeta$  and  $\hat{F}_0$  shall be known as *a priori* in the application, and the mass ratio  $\mu$  and horizontal length ratio  $p$  depend on the choices of the designer, the parameters remained to be optimized are actually  $\nu$ ,  $\eta$  and  $\beta_1$ .

In order to have better idea of how  $\eta$  and  $\beta_1$  affect the performance of TLCDs, the value of  $\nu$  is firstly assumed to be given by the designer. In fact, the value of  $\nu$  is normally up to the choice of the designer in the consideration of the provided space because it is linked to the horizontal column length of a TLCD (see Section 5 for detailed discussion). Illustrated in Fig. 4 is the distribution surface of  $[\hat{x}_p]_{\text{norm}}$  for a damped structure. Because of the smoothness of the distribution, any numerical optimization techniques such as the gradient method can be used to locate the optimal parameters  $\eta$  and  $\beta_1$ . In this paper, the program “fminsearch” in the software MATLAB was used.

From the results of extensive numerical optimization, it was indicated that the minimal  $[\hat{x}_p]_{\text{norm}}$  (i.e., the optimal case) always occurs when the two resonant peaks are equal, and this applies to both damped and undamped structures. To demonstrate this observation, the plots of  $[\hat{x}_0]_{\text{norm}}$  and  $[\hat{y}_0]_{\text{norm}}$  versus the non-dimensional excitation frequency  $k$  are shown in Figs. 5 and 6 for a damped structure ( $\nu = 2$ ,  $\zeta = 2\%$ ,  $\mu = 1\%$ ,  $p = 0.8$  and  $\hat{F}_0 = 0.01$ ) and an undamped structure ( $\nu = 2$ ,  $\zeta = 0$ ,  $\mu = 1\%$ ,  $p = 0.8$  and  $\hat{F}_0 = 0.01$ ), respectively. The plots for the optimal case ( $\beta_{1\text{opt}} = 1.0105$ ,  $\eta_{\text{opt}} = 25.436$  in Fig. 5 and  $\beta_{1\text{opt}} = 1.0080$ ,  $\eta_{\text{opt}} = 13.0810$  in Fig. 6) were denoted by the black solid curves, while the other two curves represent the cases using other values of  $\eta$  but keeping  $\beta_1$  optimal. In the optimal case, the frequencies at  $k_1$ ,  $k_2$  and  $k_3$  as denoted in Fig. 5(a) and (b) are three important frequencies that provide useful information on the excitation frequencies where the worst cases occur. They will be given in the lists of design tables presented in Section 6.

The extensive numerical results further reveal several important findings, which are described in the following:

- (1) For an undamped structure, by varying the value of  $\eta$  but keeping  $\beta_1$  the same, there exist two invariant points in  $|\hat{x}_0|$  plot and one invariant point in  $|\hat{y}_0|$  plot. As shown in Fig. 6, the two invariant points in the  $|\hat{x}_0|$  plot even share the same

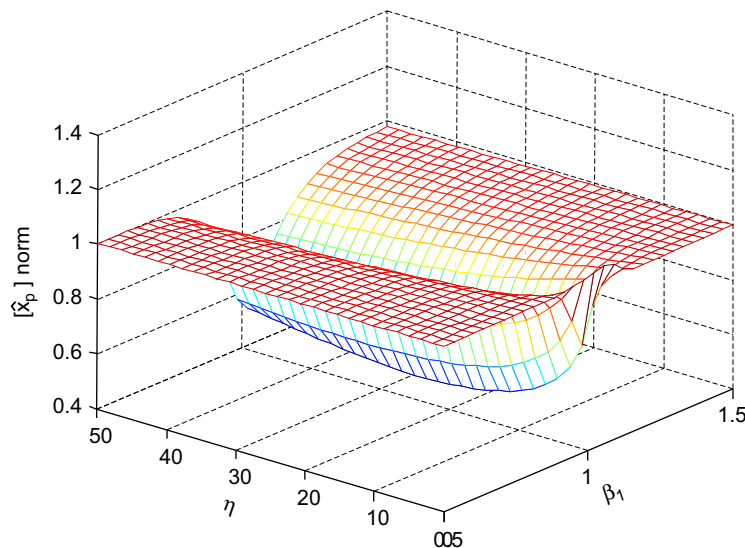
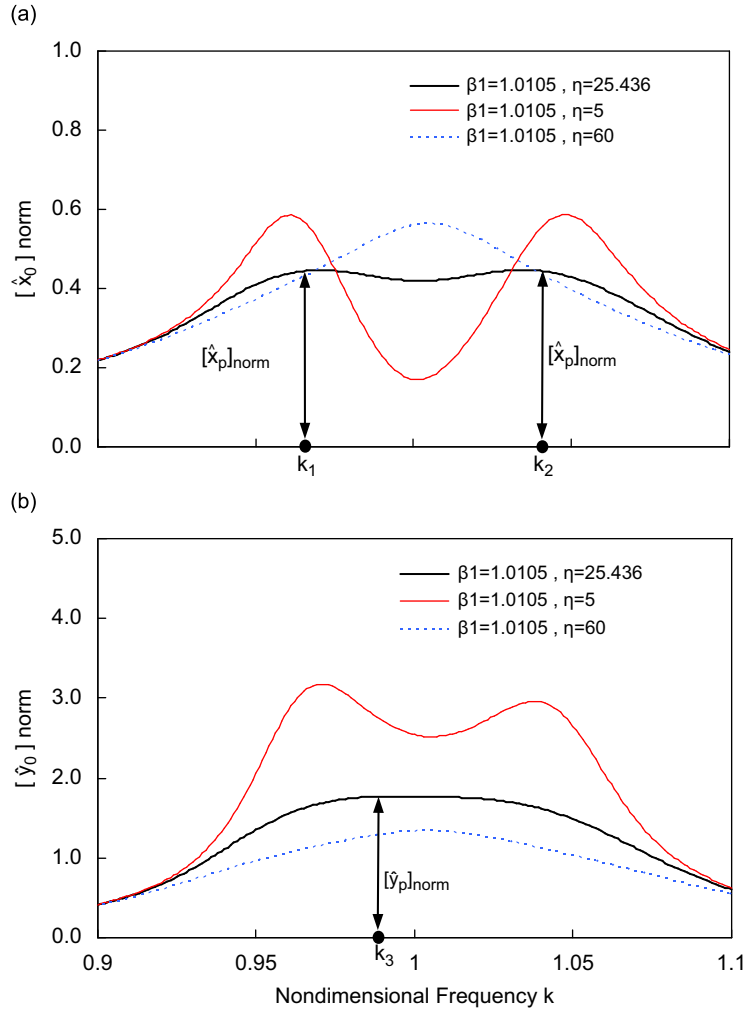


Fig. 4. Distribution surface of  $[\hat{x}_p]_{\text{norm}}$  on the  $\eta$ - $\beta_1$  plane for a case with parameters  $\nu = 2$ ,  $\zeta = 2\%$ ,  $\mu = 1\%$ ,  $p = 0.8$ , and  $\hat{F}_0 = 0.01$ .



**Fig. 5.** Demonstrative plots of  $[\hat{x}_0]_{\text{norm}}$  and  $[\hat{y}_0]_{\text{norm}}$  for a damped case (with parameters  $\nu = 2, \zeta = 2\%, \mu = 1\%, p = 0.8, \hat{F}_0 = 0.01$ ): (a)  $[\hat{x}_0]_{\text{norm}}$  versus  $k$  and (b)  $[\hat{y}_0]_{\text{norm}}$  versus  $k$ .

amplitude when the optimal  $\beta_1$  is adopted, which is actually the criterion used in the Den Hartog approach for determining the optimal tuning ratio for TMDs [15].

- (2) The optimal head loss is inversely proportional to external force amplitude, which, however, has no effect on the optimal tuning ratio  $\beta_1, [\hat{x}_p]_{\text{norm}}$  and  $[\hat{y}_p]_{\text{norm}}$ . In fact, this can be observed theoretically. Because of the co-occurrence of  $\eta|\hat{y}_0|$  in Eqs. (12)–(15), the values of  $|\hat{y}_0|$  and  $|\hat{x}_0|$  solved from Eq. (14) (or Eq. (16)) and Eq. (13) are proportional to  $\hat{F}_0$  as long as  $\eta|\hat{y}_0|$  remains constant. Thus, the external force amplitude  $\hat{F}_0$  has no effect on the optimal tuning ratio  $\beta_{1\text{opt}}$  and the associated values of  $[\hat{x}_p]_{\text{norm}}, [\hat{y}_p]_{\text{norm}}, \zeta_e, k_1, k_2$  and  $k_3$ . A constant value of  $\eta|\hat{y}_0|$  implies that the optimal head loss coefficient  $\eta_{\text{opt}}$  is inversely proportional to the force amplitude  $\hat{F}_0$ .
- (3) In case that the parameter  $\nu$  is also to be optimized, then the optimal case always occurs at  $\nu = 1$  under the same values of  $\zeta, \mu$  and  $p$ . For demonstration, the curves of minimal  $[\hat{x}_p]_{\text{norm}}$  by varying  $\nu$  in three different cases of  $\zeta, \mu$  and  $p$  are shown in Fig. 7. As observed in Fig. 7, the minimal  $[\hat{x}_p]_{\text{norm}}$  indeed occurs at  $\nu = 1$ , which indicates that using uniform cross-sections for the liquid columns is always the best choice under the same condition of structural damping, mass ratio and horizontal length ratio of the TLCD.
- (4) The optimal performance is the same for the cases with reciprocal cross-sectional ratios. Suppose that  $\nu_1$  and  $\nu_2$  are related by  $\nu_2 = 1/\nu_1$ , then it implies

$$\eta_2 = \frac{\nu_1 n_1^2}{\nu_2 n_2^2} \eta_1 \tag{25}$$

and

$$|\hat{y}_{02}| = \frac{n_2}{n_1} |\hat{y}_{01}| \tag{26}$$



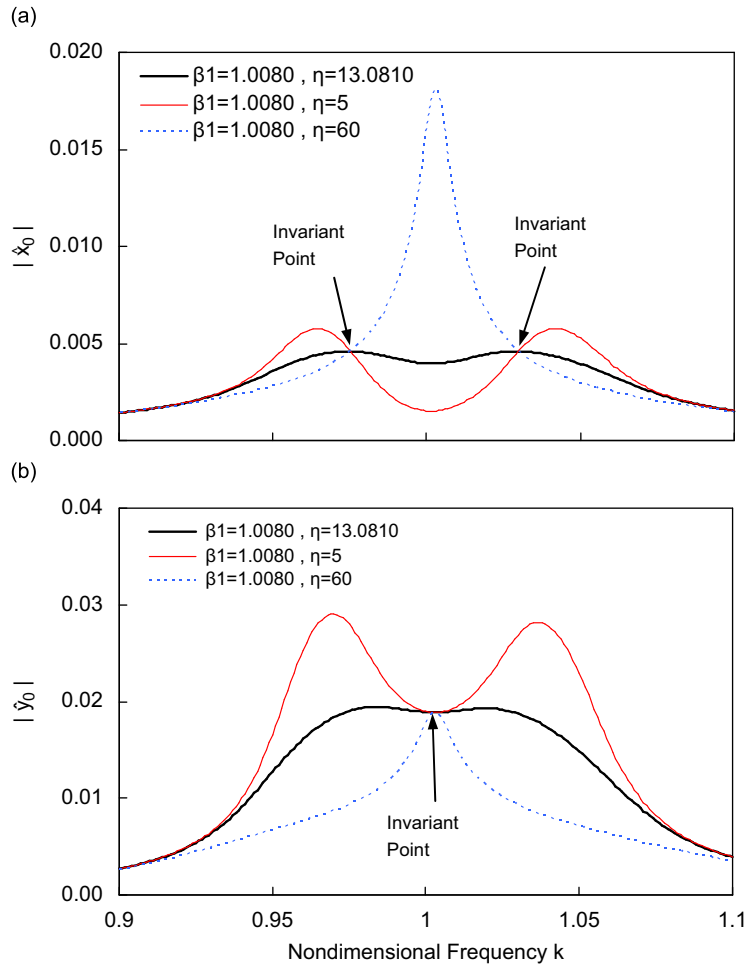


**Fig. 6.** Demonstrative plots of  $|\hat{x}_0|$  and  $|\hat{y}_0|$  for an undamped case (with parameters  $\nu = 2, \xi = 0, \mu = 1\%, p = 0.8, \hat{F}_0 = 0.01$ ): (a)  $|\hat{x}_0|$  versus  $k$  and (b)  $|\hat{y}_0|$  versus  $k$ .

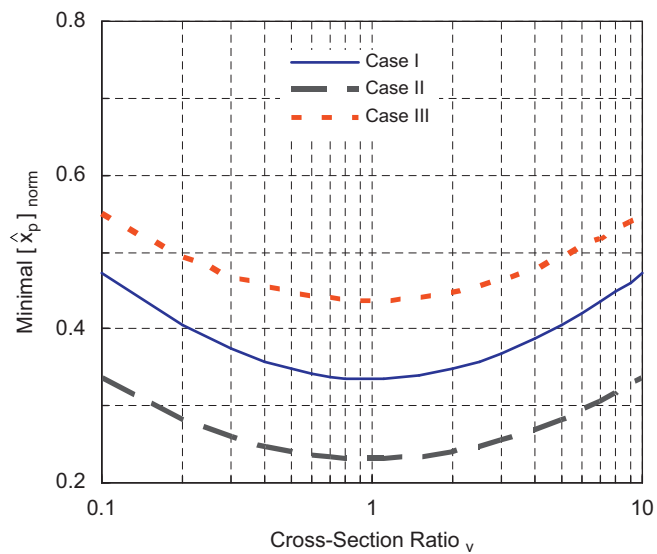


**Fig. 7.** Effect of  $\nu$  on the minimal  $[\hat{x}_p]_{\text{norm}}$  for three cases: Case I:  $\xi = 1\%, \mu = 1\%$  and  $p = 0.6$ ; Case II:  $\xi = 1\%, \mu = 2\%$  and  $p = 0.7$ ; and Case III:  $\xi = 2\%, \mu = 1\%$  and  $p = 0.8$ .

These two relations can be constructed according to the following theoretical observation. Due to the fact that (i)  $m \cdot n = p^2/[1 + (1/\nu + \nu - 2)p(1 - p)]$  is the same for both cases, and hence  $T_B$  and  $T_D$  are the same if  $\beta_1$  is the same; (ii) the co-occurrence of  $\nu n \eta |\dot{y}_0|$  in the formulation (see Eqs. (12)–(15)); and (iii)  $T_A$  is proportional to  $n^2$ , therefore the solution of  $|\dot{y}_{02}|$  in Eq. (16) is equal to  $n_2/n_1$  multiplied by  $|\dot{y}_{01}|$  if and only if  $\nu_2 n_2 \eta_2$  is equal to  $\nu_1 n_1 \eta_1 / (n_2/n_1)$ . Accordingly,  $|\dot{x}_{02}|$  should be equal to  $|\dot{x}_{01}|$  by Eq. (13). In consequence, the optimization process will just keep the optimal parameters, such as the optimal tuning ratio  $\beta_{1\text{opt}}$  and the associated values of  $[\dot{x}_p]_{\text{norm}}$ ,  $\zeta_e$ ,  $k_1$ ,  $k_2$  and  $k_3$  unchanged. The same  $[\dot{x}_p]_{\text{norm}}$  implies the same performance.

## 5. Optimal design tables

In this section, design tables containing the lists of the optimal parameters for uniform ( $\nu = 1$ ) and non-uniform ( $\nu = 2$  and  $\frac{1}{2}$ ) TLCDs were presented in Tables 1–3, 4–6 and 7, respectively, as quick guidelines for practical use. More design tables for other configurations in  $\nu$  can be referred to URL address: <http://www.ce.tku.edu.tw/~jcwu/research/tlcd.html> in readers' interest. Aside from the optimal parameters  $\beta_{1\text{opt}}$  and  $\eta_{\text{opt}}$ , the associated values of  $[\dot{x}_p]_{\text{norm}}$ ,  $[\dot{y}_p]_{\text{norm}}$ ,  $\zeta_e$  and  $k_1$ ,  $k_2$  and  $k_3$  as defined in Section 4 were all tabulated as the necessary information for design. It can be observed from Fig. 4 that the performance is not sensitive in the vicinity of  $\eta_{\text{opt}}$ . Therefore, in order to take into account the possible uncertainty existing in practice, some efforts have been made to include the range of  $\eta$  that corresponds to 5% degradation from the optimal case, as shown in Column (3) of Tables 1–6. These values of  $\eta$  are expressed as “95%” in the same columns of  $\eta_{\text{opt}}$ .

To make the design tables more complete and useful for practical use, they were also incorporated with the optimal parameters for TLCDs under a white-noise type of loading, which were excerpted from a previously published research by the authors [11]. In Wu et al. [11], due to the random nature in the responses, the rms value of the structural displacement was defined as the performance index for optimal evaluation. To design TLCDs for structures subjected to a white-noise type of loading, the readers can refer to that paper for detailed discussion.

The parametric studies according to Tables 1–6 ( $\nu \geq 1$ ) also indicated that (i) an increase in mass ratio  $\mu$  induces an increase in optimal head loss  $\eta_{\text{opt}}$  but a decrease in optimal tuning ratio  $1/\beta_{1\text{opt}} (= \omega_d/\omega_s)$ , and also induces a better performance while the two resonant peaks are increasingly apart; (ii) an increase in horizontal length ratio  $p$  induces an increase in optimal head loss  $\eta_{\text{opt}}$  but a decrease in optimal tuning ratio  $1/\beta_{1\text{opt}} (= \omega_d/\omega_s)$ , and also induces a better performance while the two resonant peaks are increasingly apart.

In the space-restricted area, there are two ways to shorten the horizontal space requirement for TLCDs, that is, by either choosing  $\nu$  larger than 1 or  $p$  as small as 0.5–0.6 or both. As observed from the design tables (such as  $\nu = 2$  in Tables 4–6), choosing a  $\nu$  larger than 1 is more preferable in that the performance downgraded is less.

Choosing  $\nu$  smaller than 1 is rarely suggested because it will elongate the horizontal liquid column length. However, in the situation when a higher frequency is tuned, the resulting short horizontal liquid column length might be too close to the dimension of TLCD cross-sections. In that case, the solution is to choose  $\nu$  smaller than 1. According to point (4) described in Section 4, the design tables for  $\nu$  smaller than 1 can be directly modified from those for  $\nu$  larger than 1 if the values of  $\nu$  are reciprocal to each other. Thus, the Columns (3) and (5) in Tables 1–3 for the case of  $\nu = 2$  can be modified to be those for the case of  $\nu = \frac{1}{2}$  by using Eqs. (25) and (26). For example, the optimal parameters for  $\nu = \frac{1}{2}$  and  $\zeta = 1\%$  was tabulated in Table 7. The results for other damping cases shall be accordingly generated, although they were not presented in the paper due to page limitation. It should be noted that the results of parametric studies in Table 7 (i.e.,  $\nu < 1$ ) basically follows the same trend as mentioned previously for Tables 1–6 (i.e.,  $\nu \geq 1$ ) except that the value of  $\eta_{\text{opt}}$  does not necessarily increase with the horizontal length ratio  $p$ .

## 6. A design example

To demonstrate the use of the design tables presented, a 75-story building used in Chang et al. [9] is adopted as the example for TLCD designs under harmonic loading. The first mode properties of this building are  $M = 4.61 \times 10^7 \text{ N s}^2/\text{m}$ ,  $C = 1.04 \times 10^6 \text{ N s/m}$  (corresponding to  $\zeta = 1\%$ ) and  $K = 5.83 \times 10^7 \text{ N/m}$  ( $\omega_s = 0.179 \cdot 2\pi \text{ rad/s}$  accordingly). Given the harmonic load in a magnitude  $F_0 = 5.0 \times 10^5 \text{ N}$ , the step-by-step procedures for TLCD designs are stated as follows:

- (1) The first trial is to choose a uniform TLCD ( $\nu = 1$ ) because the performance is the best. With a horizontal length ratio  $p$  chosen as 0.7 and a mass ratio  $\mu$  as 0.01, the optimal tuning ratio  $1/\beta_{1\text{opt}} = \omega_d/\omega_s$  is 0.9915 according to Table 1. Therefore, the total length of the TLCD,  $L$ , is 15.779 m by following  $\omega_d = \sqrt{2g/L} = \omega_s \cdot (1/\beta_{1\text{opt}}) = 1.1151 \text{ rad/s}$  (i.e.,  $T_d = 5.6346 \text{ s}$ ). The horizontal length  $L_h$  can be obtained as 11.045 m. Suppose that this horizontal length exceeds the space limit, say 10 m, then the second option is to use non-uniform TLCD design. If a cross-sectional ratio  $\nu = 2$  is picked, the frequency tuning ratio  $1/\beta_{1\text{opt}} = \omega_d/\omega_s$  is 0.9918 according to Table 4. Therefore, the effective length of the TLCD,  $L_e$ , is 15.7674 m by following  $\omega_d = \sqrt{2g/L_e} = \omega_s \cdot (1/\beta_{1\text{opt}}) = 1.1155 \text{ rad/s}$  (i.e.,  $T_d = 5.6326 \text{ s}$ ). By the relation  $L_h = L_e \cdot n = L_e \cdot p/(1 - p(1 - \nu))$ , the horizontal length  $L_h$  can be obtained as 6.4925 m, which can be allowed to be installed within the space limit. The total length  $L (= L_h/p)$  is 9.2750 m.

**Table 1**  
Optimal parameters for TLCD designs with  $\nu = 1$  and  $\zeta = 1\%$ .

$p$	$\frac{1}{\beta_{1\text{opt}}} = \frac{\omega_d}{\omega_s}$	Harmonic loading				
		$\eta_{\text{opt}} (\times 10^{-2} / \hat{F}_0)$ 95–100–95 percent	$[\hat{x}_p]_{\text{norm}}$	$[\hat{y}_p]_{\text{norm}}$	$\zeta_e$ (percent)	$k_{1,2,3} = \omega_{1,2,3} / \omega_d$
(1)	(2)	White-noise loading				
		$\eta_{\text{opt}} (\times \sqrt{10^{-4}} / S_F)$ 95–100–95 percent	$E[\hat{x}^2]_{\text{norm}}$	$E[\hat{y}^2]_{\text{norm}}$	$\zeta_e$ (percent)	–
		(3)	(4)	(5)	(6)	(7)
$\nu = 1, \zeta = 1\%, \mu = 0.01$						
0.5	0.9930 <b>0.9942</b>	6.073–9.519–12.543 <b>1.702–3.474–7.445</b>	0.379 <b>0.490</b>	2.640 <b>20.626</b>	2.64 <b>2.04</b>	0.981, 1.021, 0.994 –
0.6	0.9923 <b>0.9939</b>	6.898–10.687–13.765 <b>1.853–3.623–7.369</b>	0.334 <b>0.437</b>	2.343 <b>18.954</b>	2.99 <b>2.29</b>	0.978, 1.025, 0.992 –
0.7	0.9915 <b>0.9935</b>	7.722–11.841–15.031 <b>1.987–3.771–7.398</b>	0.299 <b>0.395</b>	2.108 <b>17.478</b>	3.34 <b>2.53</b>	0.974, 1.029, 0.990 –
0.8	0.9906 <b>0.9931</b>	8.535–12.849–16.320 <b>2.110–3.918–7.482</b>	0.271 <b>0.360</b>	1.922 <b>16.184</b>	3.69 <b>2.78</b>	0.971, 1.033, 0.987 –
0.9	0.9897 <b>0.9926</b>	9.365–14.023–17.632 <b>2.225–4.063–7.597</b>	0.247 <b>0.330</b>	1.760 <b>15.047</b>	4.05 <b>3.03</b>	0.968, 1.037, 0.985 –
$\nu = 1, \zeta = 1\%, \mu = 0.02$						
0.5	0.9866 <b>0.9886</b>	15.465–23.523–30.091 <b>3.983–7.545–14.769</b>	0.299 <b>0.392</b>	1.498 <b>8.776</b>	3.35 <b>2.55</b>	0.974, 1.029, 0.989 –
0.6	0.9854 <b>0.9880</b>	17.773–26.563–33.740 <b>4.323–7.955–15.033</b>	0.260 <b>0.345</b>	1.316 <b>7.885</b>	3.85 <b>2.90</b>	0.970, 1.035, 0.986 –
0.7	0.9839 <b>0.9873</b>	20.052–29.275–37.467 <b>4.632–8.351–15.396</b>	0.231 <b>0.308</b>	1.178 <b>7.146</b>	4.34 <b>3.25</b>	0.965, 1.042, 0.982 –
0.8	0.9822 <b>0.9865</b>	22.494–33.127–41.220 <b>4.917–8.731–15.805</b>	0.207 <b>0.278</b>	1.055 <b>6.527</b>	4.84 <b>3.60</b>	0.961, 1.047, 0.981 –
0.9	0.9804 <b>0.9856</b>	24.873–36.385–45.016 <b>5.183–9.096–16.234</b>	0.187 <b>0.253</b>	0.960 <b>6.004</b>	5.34 <b>3.95</b>	0.957, 1.053, 0.978 –
$\nu = 1, \zeta = 1\%, \mu = 0.03$						
0.5	0.9805 <b>0.9831</b>	26.998–40.511–51.051 <b>6.528–11.979–22.557</b>	0.257 <b>0.340</b>	1.066 <b>5.242</b>	3.89 <b>2.94</b>	0.970, 1.036, 0.986 –
0.6	0.9786 <b>0.9823</b>	31.289–46.472–57.869 <b>7.083–12.697–23.246</b>	0.223 <b>0.296</b>	0.928 <b>4.657</b>	4.49 <b>3.38</b>	0.964, 1.043, 0.983 –
0.7	0.9765 <b>0.9812</b>	35.596–52.253–64.770 <b>7.589–13.383–24.017</b>	0.196 <b>0.263</b>	0.823 <b>4.185</b>	5.10 <b>3.80</b>	0.959, 1.050, 0.979 –
0.8	0.9741 <b>0.9800</b>	39.966–58.169–71.748 <b>8.055–14.030–24.814</b>	0.175 <b>0.236</b>	0.739 <b>3.798</b>	5.71 <b>4.24</b>	0.954, 1.058, 0.976 –
0.9	0.9714 <b>0.9788</b>	44.378–64.132–78.790 <b>8.490–14.648–25.614</b>	0.158 <b>0.214</b>	0.671 <b>3.475</b>	6.33 <b>4.67</b>	0.950, 1.067, 0.973 –
$\nu = 1, \zeta = 1\%, \mu = 0.04$						
0.5	0.9744 <b>0.9778</b>	40.181–59.503–74.714 <b>9.261–16.677–30.701</b>	0.231 <b>0.305</b>	0.838 <b>3.619</b>	4.34 <b>3.28</b>	0.966, 1.041, 0.983 –
0.6	0.9721 <b>0.9766</b>	46.835–68.936–85.288 <b>10.048–17.735–31.872</b>	0.199 <b>0.265</b>	0.725 <b>3.193</b>	5.03 <b>3.77</b>	0.960, 1.050, 0.980 –
0.7	0.9693 <b>0.9753</b>	53.524–78.000–95.976 <b>10.765–18.734–33.097</b>	0.175 <b>0.234</b>	0.641 <b>2.854</b>	5.74 <b>4.27</b>	0.954, 1.058, 0.976 –
0.8	0.9661 <b>0.9738</b>	60.220–86.624–106.753 <b>11.426–19.675–34.325</b>	0.156 <b>0.209</b>	0.575 <b>2.580</b>	6.44 <b>4.78</b>	0.949, 1.068, 0.972 –
0.9	0.9626 <b>0.9721</b>	67.114–96.218–117.689 <b>12.040–20.564–35.526</b>	0.140 <b>0.189</b>	0.521 <b>2.353</b>	7.15 <b>5.29</b>	0.944, 1.078, 0.970 –
$\nu = 1, \zeta = 1\%, \mu = 0.05$						
0.5	0.9685 <b>0.9725</b>	54.867–81.047–100.689 <b>12.141–21.586–39.134</b>	0.212 <b>0.280</b>	0.693 <b>2.710</b>	4.72 <b>3.57</b>	0.963, 1.046, 0.981 –
0.6	0.9656 <b>0.9711</b>	64.132–93.760–115.500 <b>13.172–23.006–40.827</b>	0.182 <b>0.242</b>	0.599 <b>2.379</b>	5.50 <b>4.13</b>	0.956, 1.056, 0.977 –
0.7	0.9623 <b>0.9695</b>	73.509–106.811–135.576 <b>14.110–24.337–42.541</b>	0.159 <b>0.213</b>	0.527 <b>2.119</b>	6.29 <b>4.69</b>	0.950, 1.066, 0.974 –
0.8	0.9584 <b>0.9676</b>	83.069–119.471–145.660 <b>14.975–25.586–44.224</b>	0.142 <b>0.190</b>	0.472 <b>1.910</b>	7.08 <b>5.26</b>	0.944, 1.077, 0.970 –
0.9	0.9541 <b>0.9655</b>	92.721–132.435–161.011 <b>15.776–26.760–45.851</b>	0.127 <b>0.172</b>	0.427 <b>1.738</b>	7.87 <b>5.81</b>	0.938, 1.088, 0.967 –

Bold values indicate under white-noise loading (from Wu et al. [11]).

Ital values indicate under harmonic loading.

**Table 2**  
Optimal parameters for TLCD designs with  $\nu = 1$  and  $\xi = 2\%$ .

$p$	$\frac{1}{\beta_{1opt}} = \frac{\omega_d}{\omega_s}$	Harmonic loading				
		$\eta_{opt} (\times 10^{-2} / \dot{F}_0)$ 95–100–95 percent	$[\dot{x}_p]_{norm}$	$[\dot{y}_p]_{norm}$	$\xi_e$ (percent)	$k_{1,2,3} = \omega_{1,2,3} / \omega_d$
(1)	(2)	White-noise loading				
		$\eta_{opt} (\times \sqrt{10^{-4}} / S_F)$ 95–100–95 percent	$E[\dot{x}^2]_{norm}$	$E[\dot{y}^2]_{norm}$	$\xi_e$ (percent)	–
		(3)	(4)	(5)	(6)	(7)
$\nu = 1, \xi = 2\%, \mu = 0.01$						
0.5	0.9920 <b>0.9939</b>	8.078–14.279–20.202 <b>1.658–4.465–13.532</b>	0.564 <b>0.691</b>	3.771 <b>24.965</b>	3.55 <b>2.89</b>	0.979, 1.024, 0.999 –
0.6	0.9912 <b>0.9936</b>	8.937–15.240–20.906 <b>1.658–4.527–12.137</b>	0.514 <b>0.640</b>	3.480 <b>24.274</b>	3.89 <b>3.13</b>	0.976, 1.027, 0.997 –
0.7	0.9903 <b>0.9931</b>	9.791–16.260–21.822 <b>2.015–4.607–11.366</b>	0.472 <b>0.595</b>	3.225 <b>23.413</b>	4.24 <b>3.36</b>	0.973, 1.032, 0.996 –
0.8	0.9893 <b>0.9927</b>	10.638–17.338–22.864 <b>2.157–4.699–10.913</b>	0.436 <b>0.555</b>	3.002 <b>22.491</b>	4.59 <b>3.60</b>	0.969, 1.036, 0.994 –
0.9	0.9881 <b>0.9922</b>	11.467–18.170–23.980 <b>2.284–4.796–10.642</b>	0.405 <b>0.520</b>	2.820 <b>21.569</b>	4.94 <b>3.85</b>	0.966, 1.040, 0.990 –
$\nu = 1, \xi = 2\%, \mu = 0.02$						
0.5	0.9854 <b>0.9882</b>	19.609–32.592–43.570 <b>4.041–9.205–22.596</b>	0.472 <b>0.592</b>	2.289 <b>11.790</b>	4.24 <b>3.38</b>	0.972, 1.032, 0.996 –
0.6	0.9839 <b>0.9876</b>	21.989–35.471–46.566 <b>4.429–9.468–21.476</b>	0.423 <b>0.538</b>	2.076 <b>11.130</b>	4.73 <b>3.72</b>	0.968, 1.038, 0.992 –
0.7	0.9823 <b>0.9868</b>	24.340–38.188–49.825 <b>4.767–9.749–20.940</b>	0.383 <b>0.492</b>	1.901 <b>10.483</b>	5.23 <b>4.07</b>	0.964, 1.044, 0.989 –
0.8	0.9804 <b>0.9859</b>	26.743–41.405–53.263 <b>5.070–10.035–20.714</b>	0.350 <b>0.454</b>	1.748 <b>9.876</b>	5.72 <b>4.41</b>	0.959, 1.050, 0.986 –
0.9	0.9783 <b>0.9850</b>	29.143–44.527–56.815 <b>5.346–10.322–20.668</b>	0.322 <b>0.421</b>	1.619 <b>9.318</b>	6.22 <b>4.75</b>	0.955, 1.056, 0.983 –
$\nu = 1, \xi = 2\%, \mu = 0.03$						
0.5	0.9790 <b>0.9827</b>	33.237–53.209–70.083 <b>6.694–14.219–32.002</b>	0.420 <b>0.532</b>	1.694 <b>7.438</b>	4.77 <b>3.76</b>	0.967, 1.038, 0.992 –
0.6	0.9770 <b>0.9818</b>	37.614–58.957–76.140 <b>7.296–14.737–31.177</b>	0.373 <b>0.478</b>	1.519 <b>6.911</b>	5.37 <b>4.18</b>	0.962, 1.046, 0.988 –
0.7	0.9746 <b>0.9807</b>	41.964–64.403–82.520 <b>7.828–15.264–30.933</b>	0.335 <b>0.434</b>	1.379 <b>6.429</b>	5.98 <b>4.61</b>	0.957, 1.053, 0.984 –
0.8	0.9719 <b>0.9794</b>	46.378–70.170–89.125 <b>8.308–15.786–30.996</b>	0.304 <b>0.397</b>	1.261 <b>5.996</b>	6.59 <b>5.04</b>	0.952, 1.061, 0.980 –
0.9	0.9690 <b>0.9780</b>	50.860–76.254–95.908 <b>8.750–16.297–31.234</b>	0.279 <b>0.366</b>	1.161 <b>5.611</b>	7.20 <b>5.46</b>	0.948, 1.070, 0.977 –
$\nu = 1, \xi = 2\%, \mu = 0.04$						
0.5	0.9728 <b>0.9773</b>	48.531–76.012–99.152 <b>9.533–19.445–41.634</b>	0.384 <b>0.489</b>	1.362 <b>5.321</b>	5.21 <b>4.09</b>	0.964, 1.044, 0.988 –
0.6	0.9702 <b>0.9760</b>	55.255–85.076–108.876 <b>10.364–20.254–41.154</b>	0.339 <b>0.437</b>	1.213 <b>4.893</b>	5.91 <b>4.58</b>	0.958, 1.053, 0.984 –
0.7	0.9672 <b>0.9746</b>	62.051–94.091–119.005 <b>11.102–21.056–41.251</b>	0.303 <b>0.394</b>	1.094 <b>4.515</b>	6.60 <b>5.08</b>	0.952, 1.062, 0.980 –
0.8	0.9637 <b>0.9730</b>	68.830–102.634–129.392 <b>11.773–21.838–41.649</b>	0.274 <b>0.359</b>	0.998 <b>4.184</b>	7.31 <b>5.57</b>	0.947, 1.072, 0.976 –
0.9	0.9599 <b>0.9712</b>	75.791–112.048–140.047 <b>12.390–22.593–42.208</b>	0.250 <b>0.330</b>	0.916 <b>3.895</b>	8.01 <b>6.06</b>	0.941, 1.081, 0.973 –
$\nu = 1, \xi = 2\%, \mu = 0.05$						
0.5	0.9668 <b>0.9720</b>	65.324–101.453–130.412 <b>12.516–24.844–51.451</b>	0.358 <b>0.457</b>	1.146 <b>4.089</b>	5.59 <b>4.38</b>	0.961, 1.049, 0.986 –
0.6	0.9636 <b>0.9705</b>	74.713–113.768–144.319 <b>13.586–25.969–51.360</b>	0.315 <b>0.406</b>	1.017 <b>3.732</b>	6.37 <b>4.91</b>	0.954, 1.059, 0.982 –
0.7	0.9599 <b>0.9688</b>	84.090–125.599–158.676 <b>14.542–27.063–51.836</b>	0.280 <b>0.365</b>	0.916 <b>3.424</b>	7.15 <b>5.48</b>	0.948, 1.069, 0.977 –
0.8	0.9558 <b>0.9668</b>	93.696–138.345–173.435 <b>15.411–28.126–52.598</b>	0.253 <b>0.331</b>	0.832 <b>3.158</b>	7.94 <b>6.04</b>	0.942, 1.080, 0.973 –
0.9	0.9512 <b>0.9646</b>	103.571–151.932–188.559 <b>16.210–29.140–53.506</b>	0.230 <b>0.303</b>	0.762 <b>2.929</b>	8.73 <b>6.60</b>	0.936, 1.092, 0.970 –

Bold values indicate under white-noise loading (from Wu et al. [11]).  
Italic values indicate under harmonic loading.

**Table 3**  
Optimal parameters for TLCD designs with  $\nu = 1$  and  $\zeta = 3\%$ .

$p$	$\frac{1}{\beta_{1opt}} = \frac{\omega_d}{\omega_s}$	Harmonic loading		$\zeta_e$ (percent)	$k_{1,2,3} = \omega_{1,2,3}/\omega_d$		
		$\eta_{opt} (\times 10^{-2}/\hat{F}_0)$ 95–100–95 percent	$[\hat{x}p]_{norm}$			$[\hat{y}p]_{norm}$	
(1)	(2)	White-noise loading		$\zeta_e$ (percent)	–		
		$\eta_{opt} (\times \sqrt{10^{-4}/S_F})$ 95–100–95 percent	$E[\hat{x}^2]_{norm}$			$E[\hat{y}^2]_{norm}$	(3)
$\nu = 1, \zeta = 3\%, \mu = 0.01$							
0.5	<i>0.9908</i> <b>0.9937</b>	9.921–19.637–30.273 <b>1.475–5.456–24.934</b>	0.671 <b>0.793</b>	4.328 <b>25.076</b>	4.47 <b>3.78</b>	0.977, 1.025, 0.999 –	
0.6	<i>0.9899</i> <b>0.9933</b>	29.936–20.439–10.878 <b>1.730–5.430–20.020</b>	0.624 <b>0.750</b>	4.088 <b>25.295</b>	4.81 <b>4.00</b>	0.974, 1.030, 0.999 –	
0.7	<i>0.9888</i> <b>0.9928</b>	11.783–21.032–30.161 <b>1.937–5.443–17.400</b>	0.583 <b>0.710</b>	3.885 <b>25.156</b>	5.15 <b>4.23</b>	0.970, 1.034, 0.998 –	
0.8	<i>0.9876</i> <b>0.9923</b>	12.668–21.931–30.715 <b>2.112–5.479–15.826</b>	0.546 <b>0.673</b>	3.681 <b>24.801</b>	5.50 <b>4.46</b>	0.967, 1.038, 0.996 –	
0.9	<i>0.9864</i> <b>0.9917</b>	13.553–23.018–31.479 <b>2.264–5.531–14.809</b>	0.514 <b>0.640</b>	3.487 <b>24.316</b>	5.84 <b>4.69</b>	0.965, 1.043, 0.995 –	
$\nu = 1, \zeta = 3\%, \mu = 0.02$							
0.5	<i>0.9839</i> <b>0.9879</b>	23.584–42.090–60.082 <b>3.892–10.863–34.440</b>	0.583 <b>0.707</b>	2.761 <b>12.692</b>	5.15 <b>4.24</b>	0.971, 1.034, 0.998 –	
0.6	<i>0.9823</i> <b>0.9872</b>	26.031–44.431–61.818 <b>4.366–10.979–30.489</b>	0.533 <b>0.657</b>	2.565 <b>12.410</b>	5.64 <b>4.57</b>	0.966, 1.040, 0.996 –	
0.7	<i>0.9804</i> <b>0.9863</b>	28.514–47.376–64.243 <b>4.761–11.145–28.288</b>	0.491 <b>0.612</b>	2.384 <b>12.026</b>	6.12 <b>4.90</b>	0.962, 1.047, 0.993 –	
0.8	<i>0.9784</i> <b>0.9854</b>	30.957–50.198–67.078 <b>5.102–11.338–26.970</b>	0.454 <b>0.573</b>	2.229 <b>11.599</b>	6.62 <b>5.24</b>	0.958, 1.053, 0.990 –	
0.9	<i>0.9761</i> <b>0.9844</b>	33.406–53.202–70.183 <b>5.406–11.547–26.154</b>	0.423 <b>0.538</b>	2.091 <b>11.162</b>	7.11 <b>5.58</b>	0.953, 1.060, 0.987 –	
$\nu = 1, \zeta = 3\%, \mu = 0.03$							
0.5	<i>0.9773</i> <b>0.9823</b>	39.336–66.812–92.675 <b>6.612–16.457–45.113</b>	0.530 <b>0.651</b>	2.095 <b>8.325</b>	5.67 <b>4.61</b>	0.966, 1.041, 0.995 –	
0.6	<i>0.9751</i> <b>0.9813</b>	43.812–72.125–97.305 <b>7.310–16.775–41.533</b>	0.480 <b>0.598</b>	1.919 <b>7.997</b>	6.27 <b>5.02</b>	0.960, 1.048, 0.992 –	
0.7	<i>0.9725</i> <b>0.9801</b>	48.283–77.471–102.735 <b>7.902–17.145–39.589</b>	0.438 <b>0.552</b>	1.771 <b>7.639</b>	6.87 <b>5.43</b>	0.955, 1.056, 0.988 –	
0.8	<i>0.9696</i> <b>0.9788</b>	52.771–83.043–108.661 <b>8.423–17.539–38.496</b>	0.403 <b>0.512</b>	1.643 <b>7.281</b>	7.47 <b>5.86</b>	0.950, 1.064, 0.985 –	
0.9	<i>0.9664</i> <b>0.9773</b>	57.290–88.702–114.934 <b>8.892–17.943–37.893</b>	0.372 <b>0.478</b>	1.533 <b>6.938</b>	8.08 <b>6.28</b>	0.946, 1.073, 0.981 –	
$\nu = 1, \zeta = 3\%, \mu = 0.04$							
0.5	<i>0.9710</i> <b>0.9768</b>	56.794–94.132–127.601 <b>9.527–22.210–56.079</b>	0.492 <b>0.609</b>	1.711 <b>6.115</b>	6.10 <b>4.93</b>	0.962, 1.047, 0.993 –	
0.6	<i>0.9681</i> <b>0.9755</b>	63.637–102.273–135.765 <b>10.458–22.769–52.803</b>	0.443 <b>0.555</b>	1.557 <b>5.804</b>	6.79 <b>5.41</b>	0.956, 1.056, 0.989 –	
0.7	<i>0.9648</i> <b>0.9740</b>	70.563–111.198–144.858 <b>11.258–23.375–51.124</b>	0.402 <b>0.509</b>	1.426 <b>5.492</b>	7.48 <b>5.89</b>	0.950, 1.064, 0.985 –	
0.8	<i>0.9611</i> <b>0.9723</b>	77.444–119.617–154.521 <b>11.968–23.997–50.285</b>	0.368 <b>0.470</b>	1.319 <b>5.194</b>	8.18 <b>6.38</b>	0.945, 1.074, 0.980 –	
0.9	<i>0.9571</i> <b>0.9704</b>	84.473–128.751–164.642 <b>12.611–24.619–49.930</b>	0.339 <b>0.436</b>	1.225 <b>4.916</b>	8.89 <b>6.88</b>	0.940, 1.085, 0.977 –	
$\nu = 1, \zeta = 3\%, \mu = 0.05$							
0.5	<i>0.9648</i> <b>0.9714</b>	75.669–122.994–164.549 <b>12.589–28.099–67.201</b>	0.464 <b>0.576</b>	1.460 <b>4.792</b>	6.47 <b>5.21</b>	0.958, 1.051, 0.991 –	
0.6	<i>0.9614</i> <b>0.9699</b>	85.225–135.045–176.802 <b>13.762–28.927–64.233</b>	0.415 <b>0.522</b>	1.320 <b>4.508</b>	7.25 <b>5.75</b>	0.952, 1.062, 0.986 –	
0.7	<i>0.9574</i> <b>0.9680</b>	94.795–146.682–190.065 <b>14.779–29.793–62.844</b>	0.375 <b>0.477</b>	1.207 <b>4.235</b>	8.02 <b>6.29</b>	0.946, 1.072, 0.981 –	
0.8	<i>0.9530</i> <b>0.9660</b>	104.564–159.431–204.072 <b>15.685–30.661–62.287</b>	0.342 <b>0.438</b>	1.110 <b>3.983</b>	8.80 <b>6.85</b>	0.940, 1.083, 0.977 –	
0.9	<i>0.9480</i> <b>0.9637</b>	114.483–172.542–218.648 <b>16.507–31.515–62.205</b>	0.314 <b>0.405</b>	1.028 <b>3.752</b>	9.59 <b>7.41</b>	0.934, 1.095, 0.973 –	

Bold values indicate under white-noise loading (from Wu et al. [11]).  
Italic values indicate under harmonic loading.

**Table 4**  
Optimal parameters for TLCD designs with  $\nu = 2$  and  $\zeta = 1\%$ .

$p$	$\frac{1}{\beta_{1opt}} = \frac{\omega_d}{\omega_s}$	Harmonic loading				
		$\eta_{opt} (\times 10^{-2} / \hat{F}_0)$ 95–100–95 percent	$[\hat{x}_p]_{norm}$	$[\hat{y}_p]_{norm}$	$\xi_e$ (percent)	$k_{1,2,3} = \omega_{1,2,3} / \omega_d$
(1)	(2)	White-noise loading				
		$\eta_{opt} (\times \sqrt{10^{-4} / S_{\hat{F}}})$ 95–100–95 percent	$E[\hat{x}^2]_{norm}$	$E[\hat{y}^2]_{norm}$	$\xi_e$ (percent)	–
		(3)	(4)	(5)	(6)	(7)
$\nu = 2, \zeta = 1\%, \mu = 0.01$						
0.5	0.9932 <b>0.9943</b>	5.837–9.241–12.208 <b>1.655–3.432–7.500</b>	0.394 <b>0.507</b>	1.933 <b>10.569</b>	2.54 <b>1.97</b>	0.982, 1.020, 0.995 –
0.6	0.9926 <b>0.9940</b>	7.564–11.778–15.264 <b>2.062–4.084–8.434</b>	0.348 <b>0.453</b>	1.609 <b>8.526</b>	2.88 <b>2.21</b>	0.979, 1.024, 0.993 –
0.7	0.9918 <b>0.9936</b>	9.721–14.961–19.086 <b>2.540–4.866–9.652</b>	0.310 <b>0.408</b>	1.350 <b>6.867</b>	3.22 <b>2.45</b>	0.975, 1.028, 0.991 –
0.8	0.9909 <b>0.9932</b>	12.444–19.008–23.898 <b>3.111–5.811–11.179</b>	0.279 <b>0.370</b>	1.136 <b>5.519</b>	3.59 <b>2.70</b>	0.972, 1.032, 0.989 –
0.9	0.9899 <b>0.9927</b>	15.907–23.920–30.011 <b>3.805–6.966–13.081</b>	0.252 <b>0.336</b>	0.962 <b>4.418</b>	3.98 <b>2.98</b>	0.969, 1.037, 0.986 –
$\nu = 2, \zeta = 1\%, \mu = 0.02$						
0.5	0.9870 <b>0.9887</b>	14.806–22.721–29.065 <b>3.877–7.426–14.726</b>	0.312 <b>0.408</b>	1.102 <b>4.532</b>	3.21 <b>2.45</b>	0.976, 1.028, 0.990 –
0.6	0.9858 <b>0.9882</b>	19.466–29.522–37.179 <b>4.816–8.939–17.065</b>	0.272 <b>0.359</b>	0.904 <b>3.571</b>	3.68 <b>2.78</b>	0.971, 1.033, 0.988 –
0.7	0.9845 <b>0.9875</b>	25.316–38.067–47.334 <b>5.923–10.747–19.963</b>	0.240 <b>0.319</b>	0.749 <b>2.823</b>	4.17 <b>3.13</b>	0.967, 1.039, 0.985 –
0.8	0.9828 <b>0.9867</b>	32.657–48.151–60.117 <b>7.249–12.927–23.518</b>	0.213 <b>0.286</b>	0.628 <b>2.234</b>	4.69 <b>3.50</b>	0.963, 1.045, 0.981 –
0.9	0.9808 <b>0.9858</b>	42.127–61.549–76.461 <b>8.864–15.589–27.894</b>	0.191 <b>0.257</b>	0.526 <b>1.766</b>	5.24 <b>3.89</b>	0.958, 1.052, 0.978 –
$\nu = 2, \zeta = 1\%, \mu = 0.03$						
0.5	0.9809 <b>0.9833</b>	25.782–38.983–49.126 <b>6.358–11.767–22.389</b>	0.269 <b>0.355</b>	0.787 <b>2.717</b>	3.72 <b>2.82</b>	0.971, 1.033, 0.987 –
0.6	0.9793 <b>0.9826</b>	34.121–50.796–63.545 <b>7.892–14.245–26.293</b>	0.233 <b>0.310</b>	0.642 <b>2.116</b>	4.29 <b>3.23</b>	0.966, 1.041, 0.984 –
0.7	0.9773 <b>0.9816</b>	44.654–66.069–81.626 <b>9.704–17.199–31.057</b>	0.205 <b>0.273</b>	0.529 <b>1.658</b>	4.89 <b>3.66</b>	0.961, 1.048, 0.981 –
0.8	0.9749 <b>0.9804</b>	58.011–85.024–104.473 <b>11.877–20.757–36.859</b>	0.181 <b>0.243</b>	0.440 <b>1.302</b>	5.53 <b>4.11</b>	0.956, 1.056, 0.978 –
0.9	0.9719 <b>0.9790</b>	75.126–108.496–133.689 <b>14.521–25.096–43.973</b>	0.161 <b>0.218</b>	0.368 <b>1.023</b>	6.21 <b>4.59</b>	0.951, 1.065, 0.974 –
$\nu = 2, \zeta = 1\%, \mu = 0.04$						
0.5	0.9750 <b>0.9780</b>	38.333–57.364–71.732 <b>8.929–16.363–30.391</b>	0.242 <b>0.319</b>	0.618 <b>1.881</b>	4.14 <b>3.13</b>	0.968, 1.039, 0.985 –
0.6	0.9729 <b>0.9770</b>	51.013–75.498–93.470 <b>11.196–19.877–35.972</b>	0.208 <b>0.277</b>	0.501 <b>1.454</b>	4.80 <b>3.61</b>	0.962, 1.047, 0.981 –
0.7	0.9703 <b>0.9758</b>	66.983–97.815–120.720 <b>13.766–24.061–42.732</b>	0.182 <b>0.244</b>	0.413 <b>1.132</b>	5.50 <b>4.10</b>	0.956, 1.056, 0.977 –
0.8	0.9672 <b>0.9743</b>	87.345–126.387–155.253 <b>16.846–29.093–50.932</b>	0.161 <b>0.216</b>	0.342 <b>0.886</b>	6.23 <b>4.63</b>	0.950, 1.065, 0.974 –
0.9	0.9634 <b>0.9724</b>	113.596–162.983–199.567 <b>20.594–35.224–60.960</b>	0.143 <b>0.193</b>	0.285 <b>0.693</b>	7.01 <b>5.18</b>	0.945, 1.076, 0.970 –
$\nu = 2, \zeta = 1\%, \mu = 0.05$						
0.5	0.9692 <b>0.9728</b>	52.251–77.724–96.503 <b>11.824–21.162–38.668</b>	0.222 <b>0.293</b>	0.512 <b>1.411</b>	4.50 <b>3.41</b>	0.964, 1.043, 0.983 –
0.6	0.9666 <b>0.9716</b>	69.748–101.984–126.367 <b>14.676–25.768–46.013</b>	0.191 <b>0.254</b>	0.415 <b>1.085</b>	5.25 <b>3.94</b>	0.958, 1.052, 0.978 –
0.7	0.9635 <b>0.9700</b>	91.894–133.177–163.913 <b>18.045–31.245–54.870</b>	0.166 <b>0.222</b>	0.340 <b>0.842</b>	6.02 <b>4.50</b>	0.952, 1.062, 0.975 –
0.8	0.9596 <b>0.9682</b>	120.191–172.850–211.562 <b>22.080–37.825–65.581</b>	0.147 <b>0.197</b>	0.282 <b>0.656</b>	6.84 <b>5.08</b>	0.946, 1.074, 0.971 –
0.9	0.9550 <b>0.9660</b>	156.808–223.993–272.861 <b>26.986–45.833–78.656</b>	0.130 <b>0.175</b>	0.234 <b>0.512</b>	7.71 <b>5.71</b>	0.939, 1.086, 0.967 –

Bold values indicate under white-noise loading (from Wu et al. [11]).  
Italic values indicate under harmonic loading.

**Table 5**  
Optimal parameters for TLCD designs with  $\nu = 2$  and  $\xi = 2\%$ .

$p$	$\frac{1}{\beta_{1\text{opt}}} = \frac{\omega_d}{\omega_s}$	Harmonic loading			$\xi_e$ (percent)	$k_{1,2,3} = \omega_{1,2,3}/\omega_d$
		$\eta_{\text{opt}} (\times 10^{-2} / \hat{F}_0)$ 95–100–95 percent	$[\hat{x}_p]_{\text{norm}}$	$[\hat{y}_p]_{\text{norm}}$		
(1)	(2)	White-noise loading			$\xi_e$ (percent)	–
		$\eta_{\text{opt}} (\times \sqrt{10^{-4}/S_F})$ 95–100–95 percent	$E[\hat{x}^2]_{\text{norm}}$	$E[\hat{y}^2]_{\text{norm}}$		
		(3)	(4)	(5)	(6)	(7)
$\nu = 2, \xi = 2\%, \mu = 0.01$						
0.5	0.9922 <b>0.9940</b>	7.832–13.947–20.061 <b>1.594–4.453–14.136</b>	0.580 <b>0.707</b>	2.735 <b>12.553</b>	3.45 <b>2.83</b>	0.980, 1.022, 0.999 –
0.6	0.9915 <b>0.9937</b>	9.897–16.949–23.593 <b>2.047–5.147–14.292</b>	0.529 <b>0.656</b>	2.367 <b>10.731</b>	3.78 <b>3.05</b>	0.977, 1.026, 0.998 –
0.7	0.9906 <b>0.9933</b>	12.431–20.770–28.106 <b>2.565–5.987–15.148</b>	0.486 <b>0.610</b>	2.047 <b>9.068</b>	4.12 <b>3.28</b>	0.973, 1.030, 0.996 –
0.8	0.9896 <b>0.9928</b>	15.572–25.436–33.806 <b>3.173–7.006–16.540</b>	0.447 <b>0.567</b>	1.772 <b>7.591</b>	4.48 <b>3.53</b>	0.970, 1.034, 0.994 –
0.9	0.9883 <b>0.9923</b>	19.527–31.115–41.032 <b>3.903–8.251–18.456</b>	0.411 <b>0.527</b>	1.535 <b>6.296</b>	4.87 <b>3.80</b>	0.967, 1.040, 0.991 –
$\nu = 2, \xi = 2\%, \mu = 0.02$						
0.5	0.9858 <b>0.9884</b>	18.926–31.526–42.787 <b>3.916–9.136–23.100</b>	0.488 <b>0.609</b>	1.672 <b>5.986</b>	4.10 <b>3.28</b>	0.973, 1.030, 0.996 –
0.6	0.9844 <b>0.9878</b>	24.229–39.390–52.042 <b>4.922–10.718–24.870</b>	0.438 <b>0.555</b>	1.417 <b>4.965</b>	4.57 <b>3.61</b>	0.969, 1.036, 0.993 –
0.7	0.9829 <b>0.9871</b>	30.799–48.948–63.678 <b>6.089–12.622–27.565</b>	0.396 <b>0.507</b>	1.209 <b>4.091</b>	5.06 <b>3.94</b>	0.965, 1.042, 0.990 –
0.8	0.9810 <b>0.9862</b>	39.011–60.396–78.307 <b>7.471–14.923–31.139</b>	0.359 <b>0.465</b>	1.036 <b>3.352</b>	5.57 <b>4.30</b>	0.961, 1.048, 0.986 –
0.9	0.9788 <b>0.9852</b>	49.490–75.576–96.910 <b>9.143–17.733–35.697</b>	0.327 <b>0.427</b>	0.885 <b>2.728</b>	6.12 <b>4.69</b>	0.956, 1.055, 0.983 –
$\nu = 2, \xi = 2\%, \mu = 0.03$						
0.5	0.9795 <b>0.9830</b>	31.972–51.372–68.440 <b>6.504–14.075–32.419</b>	0.435 <b>0.549</b>	1.241 <b>3.797</b>	4.60 <b>3.64</b>	0.969, 1.036, 0.993 –
0.6	0.9776 <b>0.9821</b>	41.291–64.786–84.670 <b>8.121–16.645–35.847</b>	0.387 <b>0.495</b>	1.042 <b>3.098</b>	5.17 <b>4.04</b>	0.964, 1.043, 0.989 –
0.7	0.9754 <b>0.9810</b>	52.958–82.063–105.041 <b>10.007–19.726–40.502</b>	0.347 <b>0.448</b>	0.879 <b>2.519</b>	5.77 <b>4.46</b>	0.959, 1.051, 0.985 –
0.8	0.9727 <b>0.9798</b>	67.485–102.072–130.649 <b>12.251–23.444–46.431</b>	0.313 <b>0.408</b>	0.749 <b>2.041</b>	6.40 <b>4.91</b>	0.954, 1.059, 0.981 –
0.9	0.9696 <b>0.9783</b>	86.278–129.276–163.327 <b>14.968–27.978–53.852</b>	0.283 <b>0.372</b>	0.635 <b>1.645</b>	7.08 <b>5.38</b>	0.949, 1.068, 0.978 –
$\nu = 2, \xi = 2\%, \mu = 0.04$						
0.5	0.9735 <b>0.9776</b>	46.633–73.662–96.477 <b>9.273–19.216–41.951</b>	0.399 <b>0.507</b>	0.998 <b>2.726</b>	5.01 <b>3.95</b>	0.965, 1.041, 0.990 –
0.6	0.9711 <b>0.9765</b>	60.634–94.004–120.701 <b>11.544–22.841–47.119</b>	0.353 <b>0.453</b>	0.832 <b>2.200</b>	5.68 <b>4.41</b>	0.960, 1.050, 0.986 –
0.7	0.9682 <b>0.9751</b>	78.097–118.846–151.052 <b>14.200–27.179–53.844</b>	0.315 <b>0.408</b>	0.700 <b>1.774</b>	6.37 <b>4.90</b>	0.954, 1.059, 0.982 –
0.8	0.9648 <b>0.9735</b>	100.154–149.954–189.338 <b>17.364–32.406–62.259</b>	0.283 <b>0.369</b>	0.592 <b>1.427</b>	7.09 <b>5.42</b>	0.948, 1.068, 0.977 –
0.9	0.9607 <b>0.9716</b>	128.548–190.343–238.265 <b>21.197–38.773–72.699</b>	0.255 <b>0.335</b>	0.501 <b>1.143</b>	7.87 <b>5.97</b>	0.942, 1.079, 0.974 –
$\nu = 2, \xi = 2\%, \mu = 0.05$						
0.5	0.9676 <b>0.9723</b>	62.704–98.315–126.570 <b>12.182–24.521–51.656</b>	0.373 <b>0.474</b>	0.840 <b>2.100</b>	5.37 <b>4.22</b>	0.962, 1.046, 0.988 –
0.6	0.9647 <b>0.9710</b>	81.756–124.791–159.591 <b>15.139–29.256–58.637</b>	0.328 <b>0.422</b>	0.699 <b>1.682</b>	6.11 <b>4.74</b>	0.956, 1.055, 0.983 –
0.7	0.9612 <b>0.9694</b>	105.828–159.258–201.056 <b>18.604–34.911–67.519</b>	0.291 <b>0.378</b>	0.586 <b>1.347</b>	6.88 <b>5.29</b>	0.950, 1.066, 0.979 –
0.8	0.9571 <b>0.9674</b>	136.350–202.848–253.479 <b>22.733–41.716–78.522</b>	0.261 <b>0.341</b>	0.493 <b>1.078</b>	7.70 <b>5.87</b>	0.944, 1.077, 0.975 –
0.9	0.9521 <b>0.9651</b>	175.471–257.410–320.504 <b>27.737–49.996–92.100</b>	0.234 <b>0.308</b>	0.417 <b>0.860</b>	8.57 <b>6.49</b>	0.937, 1.089, 0.970 –

Bold values indicate under white-noise loading (from Wu et al. [11]).  
Italic values indicate under harmonic loading.

**Table 6**  
Optimal parameters for TLCD designs with  $\nu = 2$  and  $\zeta = 3\%$ .

$p$	$\frac{1}{\beta_{1opt}} = \frac{\omega_d}{\omega_s}$	Harmonic loading				
		$\eta_{opt} (\times 10^{-2} / \hat{F}_0)$ 95–100–95 percent	$[\hat{x}_p]_{norm}$	$[\hat{y}_p]_{norm}$	$\xi_e$ (percent)	$k_{1,2,3} = \omega_{1,2,3} / \omega_d$
(1)	(2)	White-noise loading				
		$\eta_{opt} (\times \sqrt{10^{-4}} / S_f)$ 95–100–95 percent	$E[\hat{x}^2]_{norm}$	$E[\hat{y}^2]_{norm}$	$\xi_e$ (percent)	–
		(3)	(4)	(5)	(6)	(7)
$\nu = 2, \zeta = 3\%, \mu = 0.01$						
0.5	<i>0.9911</i>	9.639–19.415–30.544	0.686	3.112	4.38	0.978, 1.024, 0.999
	<b>0.9938</b>	<b>1.389–5.473–27.177</b>	<b>0.806</b>	<b>12.459</b>	<b>3.72</b>	–
0.6	<i>0.9902</i>	12.071–22.825–34.245	0.639	2.765	4.70	0.975, 1.028, 0.999
	<b>0.9934</b>	<b>1.888–6.210–24.327</b>	<b>0.764</b>	<b>11.056</b>	<b>3.93</b>	–
0.7	<i>0.9892</i>	15.006–27.263–39.279	0.596	2.443	5.04	0.972, 1.033, 0.998
	<b>0.9930</b>	<b>2.446–7.108–23.718</b>	<b>0.723</b>	<b>9.648</b>	<b>4.15</b>	–
0.8	<i>0.9880</i>	18.611–32.665–45.785	0.557	2.155	5.39	0.968, 1.037, 0.997
	<b>0.9924</b>	<b>3.093–8.200–24.342</b>	<b>0.684</b>	<b>8.308</b>	<b>4.39</b>	–
0.9	<i>0.9866</i>	23.109–39.338–54.094	0.520	1.897	5.77	0.965, 1.042, 0.995
	<b>0.9918</b>	<b>3.861–9.534–25.871</b>	<b>0.646</b>	<b>7.069</b>	<b>4.64</b>	–
$\nu = 2, \zeta = 3\%, \mu = 0.02$						
0.5	<i>0.9844</i>	22.848–41.358–59.778	0.599	1.997	5.01	0.972, 1.033, 0.998
	<b>0.9881</b>	<b>3.735–10.845–36.151</b>	<b>0.723</b>	<b>6.370</b>	<b>4.15</b>	–
0.6	<i>0.9828</i>	28.850–49.998–69.884	0.548	1.736	5.48	0.967, 1.038, 0.997
	<b>0.9874</b>	<b>4.822–12.496–36.038</b>	<b>0.673</b>	<b>5.477</b>	<b>4.46</b>	–
0.7	<i>0.9811</i>	36.185–60.559–82.855	0.504	1.511	5.96	0.963, 1.044, 0.994
	<b>0.9866</b>	<b>6.058–14.495–37.807</b>	<b>0.627</b>	<b>4.651</b>	<b>4.79</b>	–
0.8	<i>0.9790</i>	45.273–73.579–99.275	0.465	1.315	6.47	0.959, 1.051, 0.991
	<b>0.9857</b>	<b>7.505–16.916–40.955</b>	<b>0.584</b>	<b>3.910</b>	<b>5.14</b>	–
0.9	<i>0.9766</i>	56.921–91.316–120.162	0.429	1.137	7.01	0.954, 1.058, 0.988
	<b>0.9846</b>	<b>9.239–19.873–45.399</b>	<b>0.544</b>	<b>3.256</b>	<b>5.51</b>	–
$\nu = 2, \zeta = 3\%, \mu = 0.03$						
0.5	<i>0.9780</i>	38.082–65.948–91.575	0.546	1.516	5.50	0.967, 1.038, 0.996
	<b>0.9826</b>	<b>6.384–16.382–46.662</b>	<b>0.668</b>	<b>4.203</b>	<b>4.49</b>	–
0.6	<i>0.9759</i>	48.439–81.062–109.347	0.495	1.302	6.07	0.962, 1.046, 0.994
	<b>0.9816</b>	<b>8.106–19.042–48.543</b>	<b>0.614</b>	<b>3.549</b>	<b>4.88</b>	–
0.7	<i>0.9734</i>	61.161–99.123–131.844	0.451	1.124	6.66	0.957, 1.053, 0.990
	<b>0.9805</b>	<b>10.081–22.250–52.478</b>	<b>0.567</b>	<b>2.968</b>	<b>5.29</b>	–
0.8	<i>0.9705</i>	77.153–122.253–160.257	0.413	0.969	7.29	0.952, 1.062, 0.986
	<b>0.9792</b>	<b>12.407–26.127–58.145</b>	<b>0.524</b>	<b>2.463</b>	<b>5.73</b>	–
0.9	<i>0.9670</i>	97.408–151.112–196.352	0.378	0.836	7.96	0.946, 1.071, 0.982
	<b>0.9776</b>	<b>15.206–30.855–65.608</b>	<b>0.484</b>	<b>2.027</b>	<b>6.20</b>	–
$\nu = 2, \zeta = 3\%, \mu = 0.04$						
0.5	<i>0.9718</i>	54.843–91.967–125.520	0.509	1.244	5.90	0.963, 1.044, 0.994
	<b>0.9772</b>	<b>9.227–22.066–57.520</b>	<b>0.626</b>	<b>3.100</b>	<b>4.79</b>	–
0.6	<i>0.9691</i>	70.128–113.738–151.934	0.458	1.062	6.56	0.958, 1.053, 0.990
	<b>0.9760</b>	<b>11.620–25.802–61.317</b>	<b>0.572</b>	<b>2.585</b>	<b>5.25</b>	–
0.7	<i>0.9660</i>	89.135–141.221–185.269	0.415	0.908	7.25	0.952, 1.062, 0.986
	<b>0.9745</b>	<b>14.381–30.293–67.446</b>	<b>0.524</b>	<b>2.140</b>	<b>5.72</b>	–
0.8	<i>0.9623</i>	113.024–175.455–227.320	0.377	0.779	7.97	0.946, 1.072, 0.982
	<b>0.9728</b>	<b>17.642–35.713–75.713</b>	<b>0.481</b>	<b>1.761</b>	<b>6.23</b>	–
0.9	<i>0.9579</i>	143.526–219.285–280.907	0.344	0.668	8.75	0.941, 1.083, 0.978
	<b>0.9708</b>	<b>21.573–42.315–86.316</b>	<b>0.443</b>	<b>1.438</b>	<b>6.78</b>	–
$\nu = 2, \zeta = 3\%, \mu = 0.05$						
0.5	<i>0.9657</i>	72.953–120.039–161.332	0.480	1.063	6.26	0.960, 1.048, 0.992
	<b>0.9719</b>	<b>12.215–27.877–68.544</b>	<b>0.594</b>	<b>2.436</b>	<b>5.05</b>	–
0.6	<i>0.9625</i>	93.715–149.061–197.253	0.430	0.903	6.99	0.954, 1.058, 0.987
	<b>0.9704</b>	<b>15.308–32.740–74.267</b>	<b>0.539</b>	<b>2.013</b>	<b>5.57</b>	–
0.7	<i>0.9588</i>	119.720–186.946–242.529	0.388	0.768	7.76	0.948, 1.069, 0.983
	<b>0.9687</b>	<b>18.891–38.572–82.644</b>	<b>0.491</b>	<b>1.654</b>	<b>6.11</b>	–
0.8	<i>0.9543</i>	152.278–232.529–299.630	0.351	0.658	8.57	0.942, 1.080, 0.978
	<b>0.9666</b>	<b>23.131–45.600–93.590</b>	<b>0.449</b>	<b>1.352</b>	<b>6.68</b>	–
0.9	<i>0.9490</i>	194.318–293.236–372.65	0.319	0.562	9.44	0.936, 1.093, 0.974
	<b>0.9642</b>	<b>28.244–54.150–107.428</b>	<b>0.411</b>	<b>1.099</b>	<b>7.29</b>	–

Bold values indicate under white-noise loading (from Wu et al. [11]).  
Italic values indicate under harmonic loading.



**Table 7**  
Optimal parameters for TLCD designs with  $\nu = 1/2$  and  $\xi = 1\%$ .

$p$	$\frac{1}{\beta_{1opt}} = \frac{\omega_d}{\omega_s}$	Harmonic loading				
		$\eta_{opt} (\times 10^{-2} / \dot{F}_0)$ 95–100–95 percent	$[\hat{x}_p]_{norm}$	$[\hat{y}_p]_{norm}$	$\xi_e$ (percent)	$k_{1,2,3} = \omega_{1,2,3} / \omega_d$
(1)	(2)	White-noise loading				
		$\eta_{opt} (\times \sqrt{10^{-4}} / S_{\dot{F}})$ 95–100–95 percent	$E[\hat{x}^2]_{norm}$	$E[\hat{y}^2]_{norm}$	$\xi_e$ (percent)	–
		(3)	(4)	(5)	(6)	(7)
$\nu = 1/2, \xi = 1\%, \mu = 0.01$						
0.5	0.9932 <b>0.9943</b>	5.837–9.241–12.208 <b>1.655–3.432–7.500</b>	0.394 <b>0.507</b>	3.866 <b>42.276</b>	2.54 <b>1.97</b>	0.982, 1.020, 0.995 –
0.6	0.9926 <b>0.9940</b>	5.791–9.018–11.686 <b>1.579–3.127–6.457</b>	0.348 <b>0.453</b>	3.678 <b>44.542</b>	2.88 <b>2.21</b>	0.979, 1.024, 0.993 –
0.7	0.9918 <b>0.9936</b>	5.684–8.749–11.162 <b>1.485–2.845–5.644</b>	0.310 <b>0.408</b>	3.530 <b>46.973</b>	3.22 <b>2.45</b>	0.976, 1.028, 0.991 –
0.8	0.9909 <b>0.9932</b>	5.530–8.448–10.621 <b>1.382–2.583–4.969</b>	0.279 <b>0.370</b>	3.409 <b>49.670</b>	3.59 <b>2.70</b>	0.972, 1.032, 0.989 –
0.9	0.9899 <b>0.9927</b>	5.331–8.017–10.059 <b>1.275–2.335–4.385</b>	0.252 <b>0.336</b>	3.322 <b>52.724</b>	3.98 <b>2.98</b>	0.969, 1.037, 0.986 –
$\nu = 1/2, \xi = 1\%, \mu = 0.02$						
0.5	0.9870 <b>0.9887</b>	14.806–22.721–29.065 <b>3.877–7.426–14.726</b>	0.312 <b>0.408</b>	2.204 <b>18.127</b>	3.21 <b>2.45</b>	0.976, 1.028, 0.990 –
0.6	0.9858 <b>0.9882</b>	14.903–22.602–28.465 <b>3.687–6.844–13.065</b>	0.272 <b>0.359</b>	2.066 <b>18.654</b>	3.68 <b>2.78</b>	0.971, 1.033, 0.988 –
0.7	0.9845 <b>0.9875</b>	14.804–22.260–27.680 <b>3.463–6.284–11.674</b>	0.240 <b>0.319</b>	1.960 <b>19.310</b>	4.17 <b>3.13</b>	0.967, 1.039, 0.985 –
0.8	0.9828 <b>0.9867</b>	14.514–21.400–26.719 <b>3.222–5.745–10.561</b>	0.213 <b>0.286</b>	1.884 <b>20.109</b>	4.69 <b>3.50</b>	0.963, 1.046, 0.981 –
0.9	0.9808 <b>0.9858</b>	14.120–20.630–25.628 <b>2.971–5.225–9.350</b>	0.191 <b>0.257</b>	1.819 <b>21.073</b>	5.24 <b>3.89</b>	0.958, 1.052, 0.978 –
$\nu = 1/2, \xi = 1\%, \mu = 0.03$						
0.5	0.9809 <b>0.9833</b>	25.782–38.983–49.126 <b>6.358–11.767–22.389</b>	0.269 <b>0.355</b>	1.573 <b>10.869</b>	3.72 <b>2.82</b>	0.971, 1.033, 0.987 –
0.6	0.9793 <b>0.9826</b>	26.124–38.891–48.652 <b>6.042–10.906–20.130</b>	0.233 <b>0.310</b>	1.467 <b>11.054</b>	4.29 <b>3.23</b>	0.966, 1.041, 0.984 –
0.7	0.9773 <b>0.9816</b>	26.112–38.636–47.733 <b>5.675–10.057–18.162</b>	0.205 <b>0.273</b>	1.383 <b>11.339</b>	4.89 <b>3.66</b>	0.961, 1.047, 0.981 –
0.8	0.9749 <b>0.9804</b>	25.782–37.788–46.433 <b>5.278–9.225–16.382</b>	0.181 <b>0.243</b>	1.319 <b>11.722</b>	5.53 <b>4.11</b>	0.956, 1.056, 0.978 –
0.9	0.9719 <b>0.9790</b>	25.180–36.366–44.810 <b>4.867–8.412–14.739</b>	0.161 <b>0.218</b>	1.271 <b>12.209</b>	6.21 <b>4.59</b>	0.951, 1.065, 0.974 –
$\nu = 1/2, \xi = 1\%, \mu = 0.04$						
0.5	0.9750 <b>0.9780</b>	38.333–57.364–71.732 <b>9.020–16.363–30.391</b>	0.242 <b>0.319</b>	1.236 <b>7.522</b>	4.14 <b>3.13</b>	0.968, 1.039, 0.985 –
0.6	0.9729 <b>0.9770</b>	39.057–57.803–71.563 <b>8.572–15.219–27.541</b>	0.208 <b>0.277</b>	1.146 <b>7.594</b>	4.80 <b>3.61</b>	0.962, 1.047, 0.981 –
0.7	0.9703 <b>0.9758</b>	39.170–57.200–70.594 <b>8.050–14.070–24.989</b>	0.182 <b>0.244</b>	1.079 <b>7.745</b>	5.50 <b>4.10</b>	0.956, 1.056, 0.977 –
0.8	0.9672 <b>0.9743</b>	38.820–56.172–69.001 <b>7.487–12.930–22.637</b>	0.161 <b>0.216</b>	1.027 <b>7.970</b>	6.23 <b>4.63</b>	0.950, 1.065, 0.974 –
0.9	0.9634 <b>0.9724</b>	38.075–54.629–66.891 <b>6.902–11.807–20.433</b>	0.143 <b>0.193</b>	0.986 <b>8.271</b>	7.01 <b>5.18</b>	0.945, 1.076, 0.970 –
$\nu = 1/2, \xi = 1\%, \mu = 0.05$						
0.5	0.9692 <b>0.9728</b>	52.251–77.724–96.503 <b>11.824–21.162–38.668</b>	0.222 <b>0.293</b>	1.025 <b>5.643</b>	4.50 <b>3.41</b>	0.964, 1.043, 0.983 –
0.6	0.9666 <b>0.9716</b>	53.401–78.082–96.750 <b>11.236–19.729–35.229</b>	0.191 <b>0.253</b>	0.949 <b>5.667</b>	5.25 <b>3.94</b>	0.958, 1.052, 0.978 –
0.7	0.9635 <b>0.9700</b>	53.737–77.879–95.852 <b>10.552–18.271–32.087</b>	0.166 <b>0.222</b>	0.890 <b>5.756</b>	6.02 <b>4.50</b>	0.952, 1.062, 0.975 –
0.8	0.9596 <b>0.9682</b>	53.418–76.822–94.028 <b>9.813–16.811–29.148</b>	0.147 <b>0.197</b>	0.845 <b>5.905</b>	6.84 <b>5.08</b>	0.946, 1.074, 0.971 –
0.9	0.9550 <b>0.9660</b>	52.559–75.078–91.458 <b>9.045–15.362–26.364</b>	0.130 <b>0.175</b>	0.810 <b>6.113</b>	7.71 <b>5.71</b>	0.939, 1.086, 0.967 –

Bold values indicate under white-noise loading (from Wu et al. [11]).  
Italic values indicate under harmonic loading.

- (2) Using the dimensionless amplitude of the external loading  $\hat{F}_0 = F_0 T_d^2 / ML_h = 0.053$ , the head loss coefficient is  $\eta_{opt} = 14.961 \cdot (10^{-2} / 0.053) = 2.8228$  according to Table 4. The 5% degradation range for the head loss coefficient  $\eta$  is from  $9.721 \cdot (10^{-2} / 0.053)$  to  $19.086 \cdot (10^{-2} / 0.053)$ , i.e., from 1.834 to 3.601.
- (3) With the choice of  $\beta_{1opt}$  and  $\eta_{opt}$ , the optimal value of  $[\hat{x}_p]_{norm} = 0.310$  occurs at  $k_1 = 0.975$  ( $\omega_1 = 1.0876$  rad/s) and  $k_2 = 1.028$  ( $\omega_2 = 1.1467$  rad/s), which are the two critical excitation frequencies that induce resonant peak amplitudes. The effective damping ratio  $\zeta_e$  of the structure equipped with the TLCD becomes 3.22%. Therefore, the damping ratio has been increased from 1% to 3.22%.
- (4) Check if the liquid surface displacement exceeds the vertical column length. From Table 4,  $[\hat{y}_p]_{norm}$  is 1.350. By Eq. (20),  $\hat{x}_{p(original)}$  is 0.066. Therefore, the worst case of  $|\hat{y}_0|$  is  $[\hat{y}_p]_{norm} \cdot \hat{x}_{p(original)} = 0.0891$  m which occurs at  $k_3 = 0.991$  (i.e.,  $\omega_3 = 1.1055$  rad/s). Since the vertical column length of the TLCD is  $L_v = (L - L_h) / 2 = 1.3913$  m which is much more than the worst case of  $|\hat{y}_0|$ , this design is feasible.
- (5) By  $\mu = \rho A_h (L_h + 2vL_v) / M$  (water  $\rho = 997$  N s<sup>2</sup>/m<sup>4</sup>), a horizontal cross-sectional area  $A_h = 38.35$  m<sup>2</sup> is thus determined. This huge cross-section is due to the large first modal mass from 75 stories in total. One possible solution to create a space for such a huge TLCD is to divide it into few smaller TLCDs with identical configurations. For instance, three identical TLCDs with a cross-section area  $A_h = 1.345 \times 9.5$  m<sup>2</sup> (1.345 m in-plane width and 9.5 m out-of-plane width) can be designed and installed on the adjacent top three floors that have similar mode shapes.

## 7. Concluding remarks

In this paper, the optimization for a TLCD installed in a single-degree-of-freedom structure subjected to harmonic loading is revisited with the aid of a proposed non-iterative analytical solution to expedite numerical computation. The results from optimization indicated that:

- The minimal  $[\hat{x}_p]_{norm}$  (optimal case) always occurs when the two resonant peak amplitudes are equal, and this applies to both damped and undamped structures.
- For an undamped structure, by varying the value of  $\eta$ , there exist two invariant points in the  $|\hat{x}_0|$  plot and one invariant point in the  $|\hat{y}_0|$  plot. When the optimal  $\beta_1$  is used, the two invariant points in  $|\hat{x}_0|$  plot even share the same amplitude, which is actually the criterion used in the Den Hartog approach for determining the optimal tuning ratio for TMDs.
- The optimal head loss is inversely proportional to external force amplitude, which however has no effect on the optimal tuning ratio  $\beta_1$  and the associated values of  $[\hat{x}_p]_{norm}$  and  $[\hat{y}_p]_{norm}$ .
- Using uniform cross-sections for the liquid columns is always the best choice under the same condition of structural damping, mass ratio and horizontal length ratio of the TLCD.
- The optimal performance is the same for the cases with reciprocal cross-section ratios. Their head loss coefficients and liquid motion amplitudes are related through Eqs. (25) and (26), respectively.

Design tables containing the lists of the optimal parameters for non-uniform (cross-section ratios 2 and  $\frac{1}{2}$ ) and uniform TLCDs were presented as quick guidelines for practical use. The parametric studies observed from the design tables indicated that:

- $v \geq 1$ : (i) an increase in mass ratio  $\mu$  induces an increase in optimal head loss  $\eta_{opt}$  but a decrease in optimal tuning ratio  $1/\beta_{1opt}(= \omega_d/\omega_s)$ , and also induces a better performance while the two resonant peaks are increasingly apart; (ii) an increase in horizontal length ratio  $p$  induces an increase in optimal head loss  $\eta_{opt}$  but a decrease in optimal tuning ratio  $1/\beta_{1opt}(= \omega_d/\omega_s)$ , and also induces a better performance while the two resonant peaks are increasingly apart.
- $v < 1$ : the same trend applies as in the case of  $v \geq 1$  except that the value of  $\eta_{opt}$  does not necessarily increase with the horizontal length ratio  $p$ .

## Acknowledgment

The authors wish to express their gratitude to National Science Council of Taiwan for the financial support under the Grant no. NSC96-2211-E-032-021.

## Appendix A. Equations of motion under external load

The kinetic energy in the structure and each part of liquid columns can be expressed as

$$T_{Structure} = \frac{1}{2} M \dot{x}^2$$

$$\begin{aligned}
 T_{\text{Left vertical column}} &= \frac{1}{2}\rho(L_v - y)A_v(\dot{y}^2 + \dot{x}^2) \\
 T_{\text{Right vertical column}} &= \frac{1}{2}\rho(L_v + y)A_v(\dot{y}^2 + \dot{x}^2) \\
 T_{\text{Horizontal column}} &= \frac{1}{2}\rho L_h A_h (v\dot{y} + \dot{x})^2
 \end{aligned} \tag{A.1}$$

and the potential energy in the structure and each part of liquid columns can be expressed as

$$\begin{aligned}
 V_{\text{Structure}} &= \frac{1}{2}Kx^2 \\
 V_{\text{Left vertical column}} &= \rho g A_v \cdot \frac{1}{2}(L_v - y)^2 \\
 V_{\text{Right vertical column}} &= \rho g A_v \cdot \frac{1}{2}(L_v + y)^2 \\
 V_{\text{Horizontal column}} &= 0
 \end{aligned} \tag{A.2}$$

in which the center line of the horizontal column is taken as the zero potential point; and  $g$  is the acceleration due to gravity. The non-conservative forces in  $x$  and  $y$  directions can be expressed as

$$Q_x = -C\dot{x} + F(t) \tag{A.3}$$

and

$$Q_y = -\frac{1}{2}\rho v \dot{y} |v \dot{y}| \eta A_h \tag{A.4}$$

Therefore, the substitution of Eqs. (A.1)–(A.4) into Lagrange's equations in  $x$  and  $y$  directions, i.e.,

$$\frac{d}{dt} \left( \frac{\partial(T-V)}{\partial \dot{x}} \right) - \frac{\partial(T-V)}{\partial x} = Q_x \quad \text{and} \quad \frac{d}{dt} \left( \frac{\partial(T-V)}{\partial \dot{y}} \right) - \frac{\partial(T-V)}{\partial y} = Q_y$$

leads to the equations of motion in Eqs. (1) and (2).

## References

- [1] F. Sakai, S. Takaeda, T. Tamaki, Tuned liquid column damper—new type device for suppression of building vibration, *Proceedings of International Conference on High-rise Buildings*, Nanjing, China, 1989, pp. 926–931.
- [2] Y.L. Xu, B. Samali, K.C.S. Kwok, Control of along-wind response of structures by mass and liquid dampers, *ASCE Journal of Engineering Mechanics* 118 (1) (1992) 20–39.
- [3] P.A. Hitchcock, K.C.S. Kwok, R.D. Watkins, Characteristics of liquid column vibration absorbers (LCVA)—I, II, *Engineering Structures* 19 (1997) 126–144.
- [4] T. Balendra, C.M. Wang, G. Rakesh, Effectiveness of TLCD on various structural systems, *Engineering Structures* 21 (4) (1999) 291–305.
- [5] K.W. Min, H.S. Kim, S.H. Lee, H. Kim, S.K. Ahn, Performance evaluation of tuned liquid column dampers for response control of a 76-story benchmark building, *Engineering Structures* 27 (7) (2005) 1101–1112.
- [6] J.L.P. Felix, J.M. Balthazar, R.M.L.R.F. Brasil, On tuned liquid column dampers mounted on a structural frame under a non-ideal excitation, *Journal of Sound and Vibration* 282 (3–5) (2005) 1285–1292.
- [7] S.D. Xue, J.M. Ko, Y.L. Xu, Tuned liquid column damper for suppressing pitching motion of structures, *Engineering Structures* 23 (11) (2000) 1538–1551.
- [8] J.C. Wu, Y.P. Wang, C.L. Lee, P.H. Liao, Y.H. Chen, Wind-induced interaction of a non-uniform tuned liquid column damper and a structure in pitching motion, *Engineering Structures* 30 (12) (2008) 3555–3565.
- [9] C.C. Chang, C.T. Hsu, Control performance of liquid column vibration absorbers, *Engineering Structures* 20 (7) (1998) 580–586.
- [10] C.C. Chang, Mass dampers and their optimal designs for building vibration control, *Engineering Structures* 21 (1999) 454–463.
- [11] J.C. Wu, M.H. Shih, Y.Y. Lin, Y.C. Shen, Design guidelines for tuned liquid column damper for structures responding to wind, *Engineering Structures* 27 (13) (2005) 1893–1905.
- [12] S. Yalla, A. Kareem, Optimum absorber parameters for tuned liquid column dampers, *ASCE Journal of Structural Engineering* 126 (8) (2000) 906–915.
- [13] E. Simiu, R.H. Scanlan, *Wind Effects on Structures*, Wiley, New York, 1996.
- [14] H. Gao, K.C.S. Kwok, B. Samali, Optimization of tuned liquid column damper, *Engineering Structures* 19 (6) (1997) 476–486.
- [15] J.P. Den Hartog, *Mechanical Vibrations*, fourth ed., McGraw-Hill, New York, 1956.
- [16] R.E. Skelton, *Dynamic Systems Control: Linear Systems Analysis and Synthesis*, Wiley, New York, 1988.